Technical Report No. 2

ELECTRICAL CONTACTS TO CADMIUM SULFIDE SINGLE CRYSTALS

Contract: No. NsG - 573
National Aeronautics
and Space Administration
Goddard Space Flight Center

Authority: (Physics Branch)

Project Director: K. W. Böer
Department of Physics
University of Delaware
Newark, Delaware

ELECTRICAL CONTACTS TO CADMIUM SULFIDE SINGLE CRYSTALS

by

Robert Burton Hall

A thesis submitted to the Faculty of the University of Delaware in partial fulfillment of the requirements for the degree of Master of Science in Physics.

June, 1966

ACKNOWLEDGEMENTS

The author wishes to express sincere appreciation to Professor K. W. Böer for his suggestion of this project and for his enlightening discussions which gave it direction and meaning.

Thanks also to Mr. Melvin Weaver and Mr. Edgar Riley for the able assistance in the construction of the apparatus, and to Mrs. Gayle O'Connell for her diligent work in the typing of the work in its final form.

TABLE OF CONTENTS

CHAPTER		PAGE
I.	Introduction	1
II.	Theoretical Considerations	3
	A. Defining terms	3
	B. The Simplified Junction Theory	3
	C. The Blocking Contact	5
	D. The Injecting Contact	9
	E. Junction-Bulk Crystal I-V Characteristics	10
	F. Junction-Bulk Crystal-Junction I-V Characteristics	20
III.	Experimental Considerations	28
	A. Previous Work	28
	B. A New Approach	30
IV.	Apparatus and Procedure	34
	A. Preparing the Contacts	34
	B. Measuring the Contact Properties	38
V.	Experimental Results	44
	A. Single Layer Electrodes	44
	B. Multi-layer Electrodes	50
VI.	Discussion and Conclusion	55
	A. Discussion of Experimental Results	55
	B. General Comments	61
	References	65

ABSTRACT

It is well known that at room temperature ohmic-behaving electrical contacts to CdS single crystals can easily be attained. However, at temperatures greater than 100°C such contacts exhibit instability (e.g., diffusion of indium into the bulk of the crystal above 100°C where, acting as a donor, it may dominate crystal behavior). A multilayer technique has been developed which permits evaporated electrodes to perform ohmically up to 300°C. This technique is characterized by the usage of a preparative metal to "clean" the surface of the crystal to be electroded, an active metal to serve as the ohmic-behaving electrical contact, and a covering metal to carry current and act as a diffusion sink. Although in half the cases a heat treatment of the multilayer-crystal system is necessary to create an ohmic-behaving contact, the results using titanium as the preparative metal and aluminum as the active metal have been completely successful.

I. INTRODUCTION

The task of creating an electrical contact on cadmium sulfide has received much attention. Previous investigations have shown that at room temperatures indium and gallium serve as ohmic contacts to CdS and thereby act as a reservoir of electrons that can be supplied to the bulk crystal as needed. In a few investigations aluminum has been used successfully as an ohmic contact - retaining its ohmicity without degradation at elevated temperatures (up to 350°C). Also, metals such as gold and silver, having work functions greater than that of CdS, have been made to serve somewhat satisfactorily as ohmic behaving electrical contacts to CdS under specialized conditions.

With the exception of aluminum, the above mentioned metals are not stable as ohmic behaving electrical contacts to cadmium sulfide. In the cases when indium and gallium are used, elevated temperatures (above 70°C) result in massive diffusion of the electrode material into the bulk where, acting as donors, they may dominate crystal characteristics. Gold, silver and other metals give ohmic contacts only after a low pressure gas discharge, but the ohmicity is usually annealed out at elevated temperatures. The difficulty of degradation of the ohmic electrodes at elevated temperatures due to electrode diffusion or disappearance of ohmicity does not occur when aluminum serves as the ohmic contact. However, since oxygen on the CdS surface reacts with aluminum forming an insulating layer, it is difficult to achieve ohmic behaving contacts with this metal. Thus far the only way to consistently achieve ohmic contacts using aluminum is by evaporation onto a vacuum cleaved crystal.

It is proposed that a multilayer technique (i.e. coevaporation in vacuum of two or more metals) would enable both aluminum and indium to act as stable ohmic contacts. The preparative metal (Au, Pt, Ti) would serve to enhance impurity desorption, and then an active metal (Al, In, Ga) would make the ohmic behaving electrical contact. A final covering metal (Au, Ag, Pt,...) would supply the bulk with electrons via the active metal contact and also act as a sink for the diffusion of any excess active metal. When aluminum is the active metal, it is necessary to use a preparative metal to "clean" the CdS surface. In the case of indium where impurity desorption is not critical, the success of the multi-layer technique does not depend on a preparative metal. In this case it is reasoned that if the deposit of the active metal, indium, is thin enough (i.e. a mono-layer), it will be trapped at the surface and thus will not readily diffuse into the bulk crystal at elevated temperatures.

II. THEORETICAL CONSIDERATIONS

A. Defining terms. In discussing the bringing of a metal into intimate contact forming a metal-semiconductor junction, several quantities must be defined. First, a work function, Φ_m, is defined as the energy necessary to move an electron from the Fermi level in the metal to the vacuum level. Second, a work function, Φ_s, is likewise defined as the energy necessary to move an electron from the Fermi level in the semiconductor to the vacuum level. However, for a semiconductor the Fermi level is dependent in any given semiconductor on concentration and energy of impurity centers. Also, lying in the forbidden gap, the Fermi level does not necessarily coincide with a allowed level there. It is thus convenient to introduce an quantity χ, the electron affinity, and define it as the energy necessary to move an electron from the lowest energy level in the conduction band of the semiconductor to the vacuum level. Usage of these terms will occur in the development of the simplified junction theory. It is now significant to consider two different cases of the metal-semiconductor junction: $\Phi_m > \Phi_s$ and $\Phi_s > \Phi_m$. For the sake of simplicity, it is assumed that in the semiconductor there: 1) are no surface states, 2) exists one well defined donor level N_D at an energy E_D (such that the semiconductor is n-type), and 3) are no effects due to image forces. These above conditions describe the assumptions for the simplified theory.

B. The Simplified Junction Theory. First, consider the case where the work function, Φ_m, of the metal is greater than the work function, Φ_s, of the semiconductor. As a

consequence of forming a junction of a metal and a semiconductor, there will be a redistribution of charges at the interface of the two materials in such a way that at thermal equilibrium the Fermi level has the same value in the complete metal-semiconductor system. As a result of this charge exchange electrons from the semiconductor will flow into the metal leaving ionized donors in the semiconductor. See Figure (1) and (2).

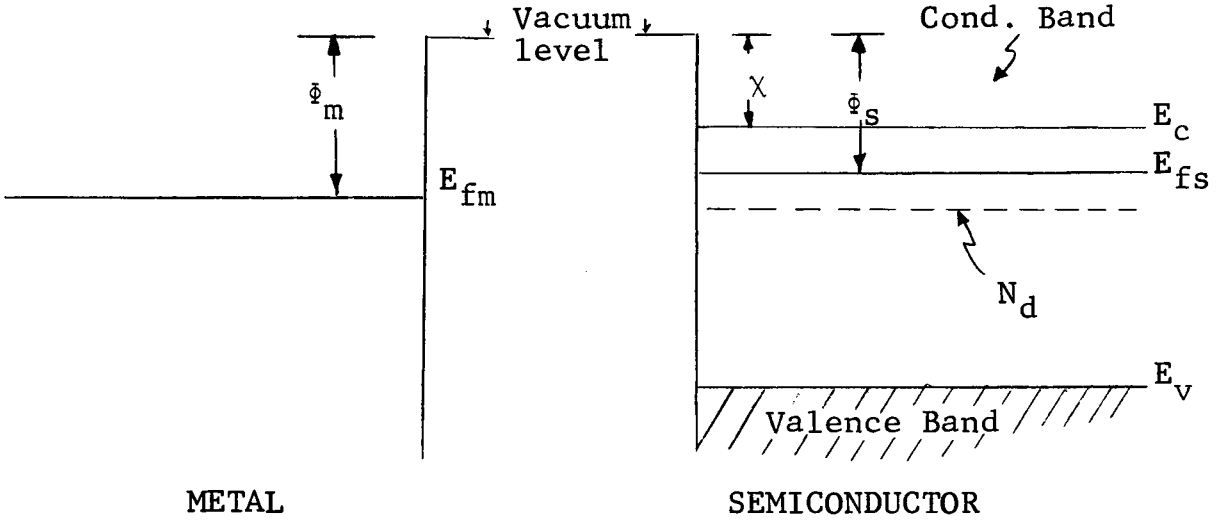

Figure (1). Energy level diagram of a metal and semiconductor before contact for case of $\Phi_m > \Phi_s$.

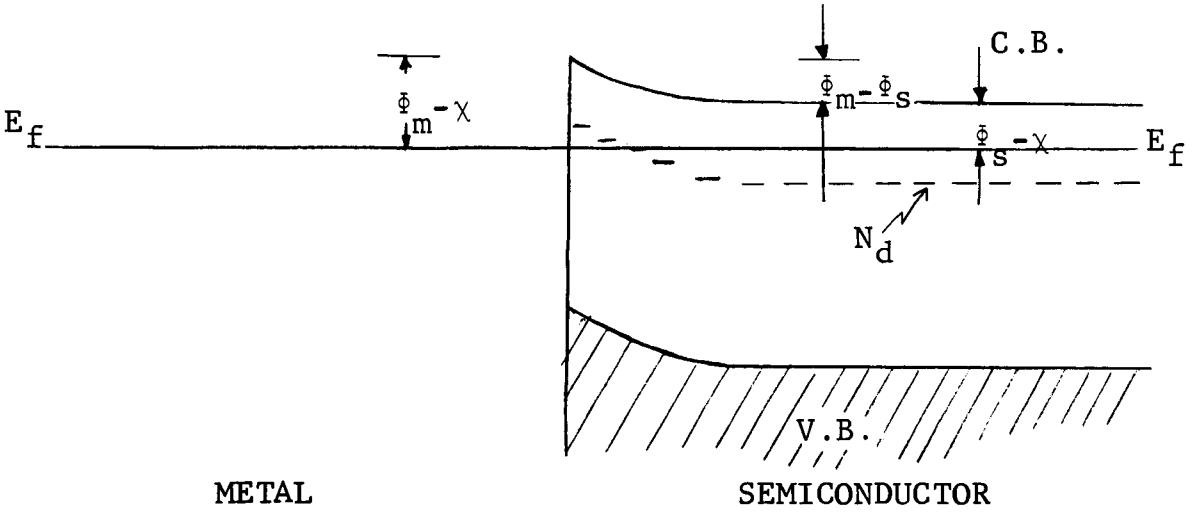

Figure (2). Energy level diagram of metal-semiconductor junction after contact for case of $\Phi_m > \Phi_s$.

The quantities defining the character of this simplified contact junction may be thought of in the following way. First, far in the bulk of the crystal, the semiconductor system is not aware that a metal has been placed at the surface; thus at $x = \infty$ the quantity $\Phi_s - \chi$ is a boundary condition. Second, at the exact junction of the two systems, for an electron to enter the semiconductor at the lowest state in the conduction band from the Fermi level in the metal, it must overcome a barrier, $\Phi_m - \chi$ (the quantity $\Phi_m - \chi$ from the Simplified Junction Theory is called the barrier height). In the region between the boundaries $\Phi_m - \chi$ and $\Phi_s - \chi$ lies a region, for the case where $\Phi_m > \Phi_s$, called the depletion region. For the case where $\Phi_m > \Phi_s$ the electrical contact at the junction of the two systems is considered "blocking".

Second, consider the case where $\Phi_s > \Phi_m$ when the semiconductor is n-type as shown in Figures (3) and (4). In this situation, the difference in the work function gives rise to a flow of electrons from the metal into the semiconductor. This time the region between the interface and the bulk semiconductor is called the accumulation region. For the simplified junction case, where $\Phi_s > \Phi_m$ and for an n-type semiconductor, the electrical contact is considered "injecting"[a].

C. The Blocking Contact. For the case of the blocking contact (i.e. where $\Phi_m \geq \Phi_s$) two considerations must be made: one for the barrier layer thickness being small compared with the mean free path of the electron (diode theory), the other for the barrier thickness being large compared to the mean free path (diffusion theory).[1]

---

[a] N.B. Actually, a third purely mathematical case, for the simplified junction exists. This occurs when $\Phi_m = \Phi_s$. There then is no charge exchange and this junction is referred to as a neutral contact.

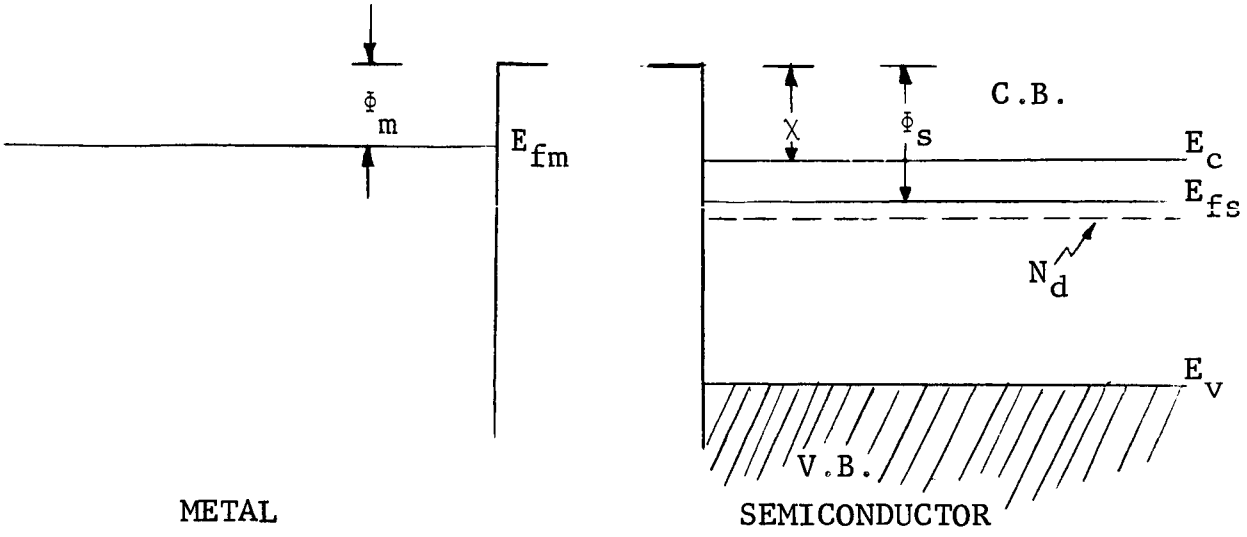

Figure (3). Energy level diagram of a metal and a semiconductor before contact for case of $\Phi_m < \Phi_s$.

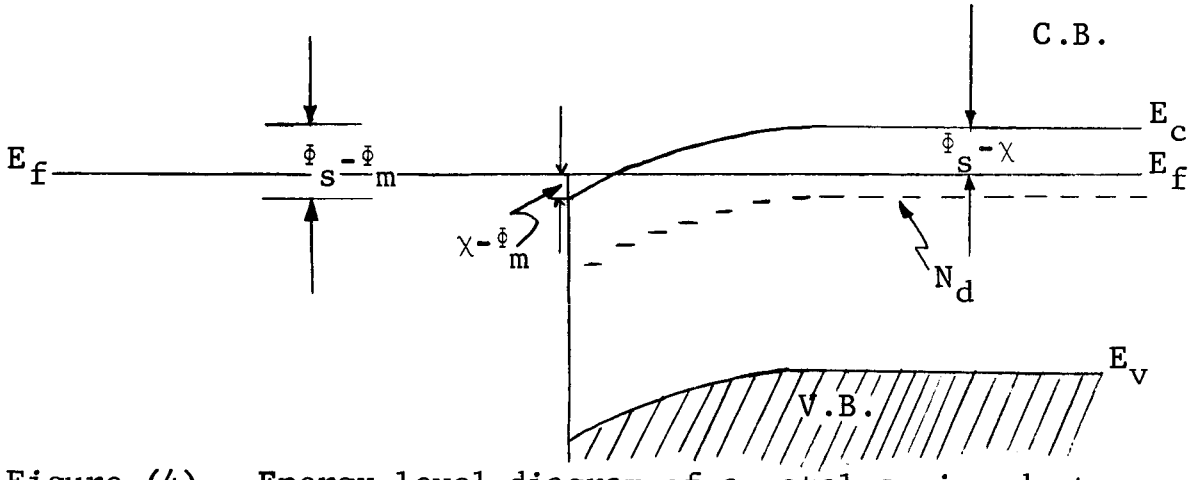

Figure (4). Energy level diagram of a metal-semiconductor junction after contact for case of $\Phi_m < \Phi_s$.

In the diode theory the particle density from the junction region in the semiconductor to the metal at the plane x = o is:

$$\overleftarrow{S} = \frac{1}{\sqrt{6\pi}} V_{th} n_B e^{-e(V_D \pm V)/kT} \qquad (1)$$

where: V_{th} ≡ thermal velocity

n_B ≡ equilibrium electron concentration in bulk semiconductor

V ≡ applied voltage at the junction

V_D ≡ diffusion voltage.

The particle current density in the other direction (metal to junction region in semiconductor) is given by

$$\vec{S} = \frac{1}{\sqrt{6\pi}} V_{th} \cdot n_o . \tag{2}$$

By subtracting equation (1) from (2) and multiplying by e gives for the non-zero case after extended mathematical development,

$$eS = e(\overleftarrow{S} - \vec{S}) = j' = j'_o \left(e^{\pm eV/kT} - 1\right) \tag{3}$$

$$\text{where: } j'_o = \frac{1}{\sqrt{6\pi}} eV_{th} n_o . \tag{3a}$$

When V is plus such that the junction is negative with respect to the metal then,

$$j' = j'_o \left(e^{+ eV/kT} - 1\right) = j'_{for.} \tag{4}$$

and for all plus values of V the current j is called the forward current, $j'_{for.}$

When V is negative such that the junction is positive with respect to the metal then,

$$j' = j'_o \left(e^{-eV/kT} - 1\right) = j'_{rev.} \tag{5}$$

and for all negative values of V the current j' is called the reverse current. It should be noted that in this case for values of $V > 4 \frac{kT}{e}$, $j'_{rev} \simeq - j'_o$ and the current saturates. Physically, this saturation corresponds to the maximum amount of current that the metal electrode can supply to the semiconductor.

For the diffusion theory it is assumed that the electrons suffer sufficient collisions with phonons and imperfections while in the barrier layer such that it is now necessary to incorporate a diffusion term. The calculation of current flow at the junction proceeds in the same manner as for the diode theory only with new expressions for $\vec{S}$ and $\overleftarrow{S}$ [See Table I]. Here then

$$e\,S = e\,(\overleftarrow{S} - \vec{S}) = j = j_o^* \quad (e^{\pm\, eV/kT} - 1) \tag{6}$$

where:

$$j_o^* = e\mu_n\, n_o E_o \tag{6a}$$

where: $\mu_n \equiv$ mobility of electron.

$n_o \equiv$ # electrons existing in the semiconductor at x = o. (i.e. right at the interface).

$E_o \equiv$ is a linearized field in the depletion region (an approximation).

TABLE I

	metal→semiconductor $\vec{S}$	semiconductor→metal $\overleftarrow{S}$
diode theory	$\frac{1}{\sqrt{6\pi}}\, V_{th}\, n_o$	$\frac{1}{\sqrt{6\pi}}\, V_{th}\, n_B\, e^{-e(V_D+V)/kT}$
diffusion theory	$D\,\frac{dn}{dx}$	$\mu_n\,\frac{dV}{dx}$

A forward and reverse current are again defined as they were for the diode theory model:

$$j_{for.} = j_o^*\,(e^{\,eV/kT} - 1) \tag{7}$$

$$j_{rev.} = j_o^*\,(e^{-eV/kT} - 1). \tag{8}$$

The j_o' term that appears in equations (5) and (6) and the j_o^*

term in equations (7) and (8) represent the emission capacity of the metal and both depend on the quantity, $\Phi_m - \chi$:

$$j_o' = \frac{1}{\sqrt{6\pi}} e V_{th} n_o \qquad (3a)$$

$$j_o^* = e \mu_n n_o E_o \qquad (6a)$$

where:

$$n_o = N_c e^{-(\Phi_m - \chi)/kT}. \qquad (9)$$

D. The Injecting Contact. The case of the injecting contact ($\Phi_m > \Phi_s$) was considered by Mott and Gurney.[2] It is possible now to use both the Poisson and current flow equation in the same development:

$$j = n(x) e \mu E - De \frac{dn(x)}{dx} \qquad (10)$$

$$\frac{dE}{dx} = \frac{n(x)e}{K\epsilon_o} . \qquad (11)$$

Eliminating n(x),

$$\frac{j}{K\epsilon_o} = \mu E \frac{dE}{dx} - D \frac{d^2E}{dx^2} . \qquad (12)$$

Integrating,

$$\frac{jx}{K\epsilon_o} + \text{const.} = \frac{1}{2} \mu E^2 - D \frac{dE}{dx} \qquad (13)$$

then substituting $D = \frac{\mu kT}{e\mu}$, and assuming that $\frac{dE}{dx} \approx \frac{E}{L}$ (where L is the distance between the electrodes) it is then possible to neglect the last term (i.e. $kT \frac{dE}{dx} << eE^2$) which will be the case if $kT << eFL$, or that the potential across the crystal is large compared with 25mv. Then equation (13) becomes,

$$E = \sqrt{\frac{2j}{K\epsilon_o \mu}\ (x + x_o)} \tag{14}$$

where $x_o = \frac{jK\epsilon_o}{2\mu N^2 e^2}$ which is evaluated at $x = 0$, where $n = n_o$. After mathematical manipulation where use is made of the assumption that $x_o \ll L$, it results that

$$j = \frac{9}{8}\ \frac{K\epsilon_o \mu V^2}{L^3}\ . \tag{15}$$

Thus the very interesting result for the injecting junction is that the current is proportional to the square of the voltage. This is the solid state analog to space charge limited currents in vacuum diodes.

E. Junction - bulk crystal I-V Characteristics. Consider now possible I-V characteristics for a single blocking contact junction and the adjacent bulk resistance of the semiconductor. From equations (3a), (6a) and (9) it turns out that

$$j_o' = \frac{1}{\sqrt{6}}\ e\ V_{th} N_c e^{-(\Phi_m - \chi)/kT} \tag{3b}$$

$$j_o^* = e\mu_n E_o N_c\ e^{-(\Phi_m - \chi)/kT} \tag{6b}$$

Evaluating part of the preceding coefficients in (3b) and (6b) gives,

$$j_o' = 1.2 \times 10^2 T^2 e^{-(\Phi_m - \chi)/kT} \tag{16}$$

$$j_o^* = 4.0\ \mu_n E_o e^{-(\Phi_m - \chi)/kT}\ . \tag{17}$$

When the values of T, μ_n, and E_o are put into equations (16) and (17), the saturation current of the reverse biased metal-semiconductor junction may be obtained. It is, for

example, worthwhile to plot $j'_{rev} = j'_o(e^{-eV/kT}-1)$ (the diode theory) for various assumed saturation values of j'_o. Then, if one plots the assumed Ohm's Law current, $j_{ohmic} = \frac{V}{R_B}$ (where $R_B = L/n_B e\mu A^2$ is the bulk resistance) on the same graph, it is now possible to discuss the profile of the metal-semiconductor junction-bulk series resistance circuit. Graph (1) shows $j'_{rev.} = j'_{rev.}(V)$ and $j_{ohmic} = j_{ohmic}(V)$ for various values of R_B and j'_o. For any choice of R_B and j'_o the current will be fixed at a given voltage in such a way as to allow the proper current to flow through the series resistance of junction plus bulk. For example, if $j'_o = 10^{-7}$ amps/cm^2 and $R_B = 10^7$ ohms, it can be seen that for this junction in the reverse biased case (i.e. voltage applied such that bulk is positive, the metal electrode negative) that at low applied voltages (below 10^0 volts) the I-V profile will be linear. At voltages between 10^0 volts and 10^2 volts a transition occurs in such a way that now the potential distribution changes, and for voltages greater than 10^2 volts the saturation limit of the junction dominates. This may be more quantitatively expressed in the following manner: the current through the junction-bulk semiconductor series is

$$j'_{rev} = \frac{V_A}{R_B + R_j} \tag{18}$$

where: $V_A \equiv$ applied voltage
$R_B \equiv$ bulk resistance
$R_j \equiv$ effective junction resistance

also,

$$\left.\begin{aligned} R_B &= \frac{V_B}{j'_{rev}} \\ R_j &= \frac{V_j}{j'_{rev}} \end{aligned}\right\} \quad V_A = V_B + V_j . \tag{19}$$

The effective junction resistance is

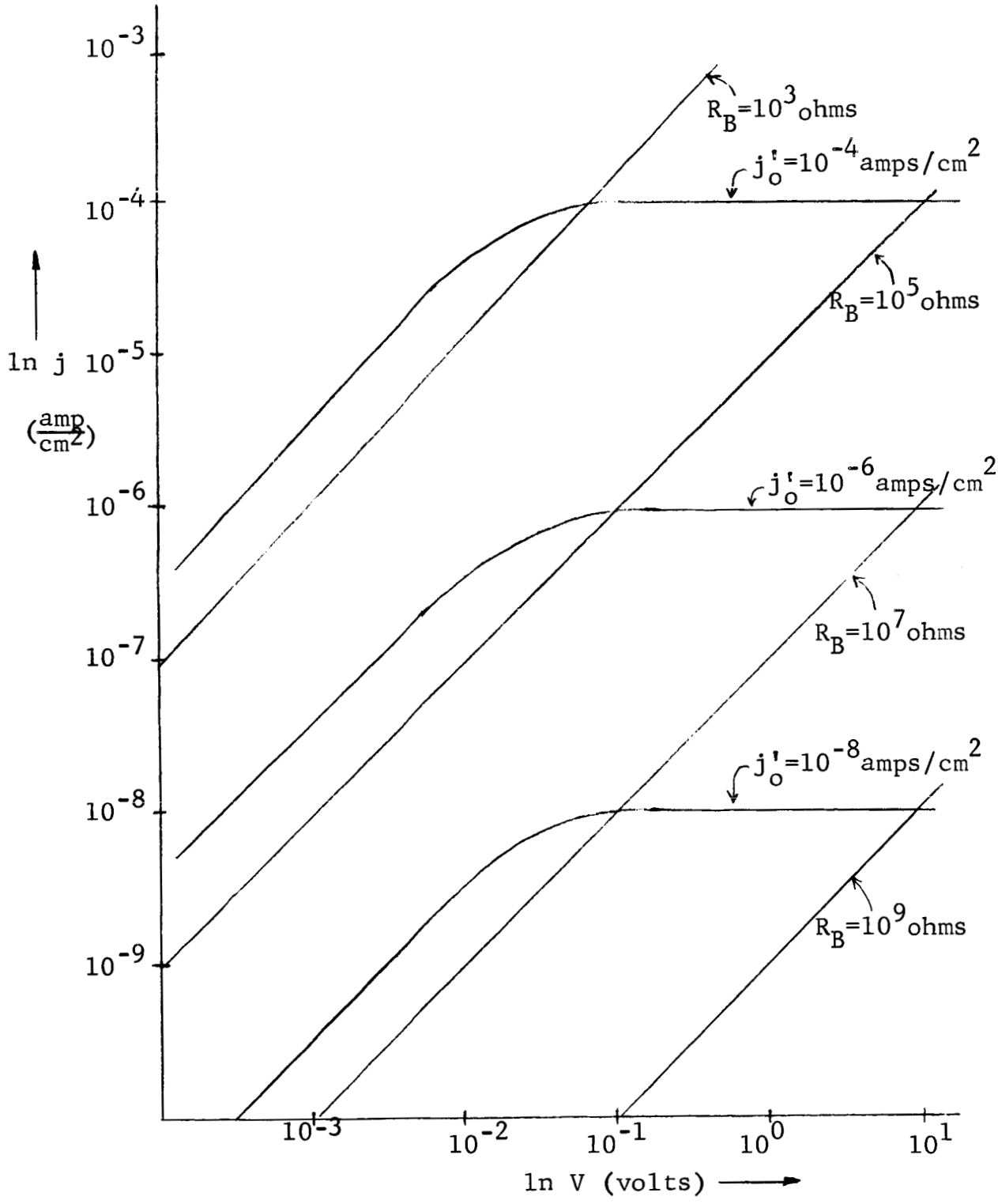

Graph (1). A family of saturation currents j_o' - (diode theory) curves and bulk resistance curves. For any choice of R_B and j_o' the current will be fixed at a given voltage in such a way as to allow the proper current to flow through the series resistance of junction plus bulk.

$$R_j = \frac{V_j}{j_o' \left(e^{-eV_j/kT} - 1\right)} \quad . \tag{20}$$

Putting equation (20) into (18) gives the current-voltage expression,

$$\left.\begin{aligned} j'_{rev} &= \frac{V_A}{R_B + \frac{V_j}{j_o'} \frac{1}{\left(e^{-eV_j/kT} - 1\right)}} \\ &= \frac{V_A}{R_B + \frac{\alpha V_A}{j_o' \left(e^{-e\alpha V_A/kT} - 1\right)}} \end{aligned}\right\} \tag{21}$$

where: $\alpha = \frac{V_j}{V_A}$ such that $0 \leq \alpha \leq 1$.

Equation (21) indicates the $j'_{rev.} = j'_{rev.}(V_A)$ curve will be dominated by whichever of the two denominator terms is largest. For low applied voltages and for the proper initial conditions on R_B and j_o', $R_B >> R_j$ and the I-V profile is linear; for high voltages $R_B << R_j$ then the I-V profile is saturated, being dominated by the junction. The transition occurs when the two terms, R_B and R_j, become approximately equal. A precise description of the I-V profile in the transition can be easily evaluated from equation (21), knowing α.

Similarly, resistance can be described for the forward biased junction. Here the current through the junction - bulk semiconductor system follows from equation (21) with the sign change in the exponential,

$$j'_{for} = \frac{V_A}{R_B + \frac{\alpha V_A}{j_o' \left(e^{+e\alpha V_A/kT} - 1\right)}} \quad . \tag{22}$$

Thus in equation (22) for low applied voltages and for the proper initial conditions on R_B and j_o', $R_B << R_j$ and the I-V profile is determined by the junction. At high applied

voltages $R_B >> R_j$, and the bulk resistance dominates the I-V curve. The transition occurs when $R_B \simeq R_j$; again knowing the value of α, it is easy to evaluate precisely the transition using equation (22).

Using equations (21) and (22), consider first the case of the blocking contact I-V profile as shown in Graph (2). (Special attention must be paid to the origin of this graph and the ones to follow since they are log-log plots). The solid line in the first and third quadrant of Graph (2) gives the resulting I-V curve profile for $j_o' = 10^{-6}$ amps/cm^2 and $R_B = 10^7$ ohms. Thus for a blocking contact with a high bulk resistance the I-V profile is linear in the forward direction, and is also linear in the reverse direction until saturation is reached.

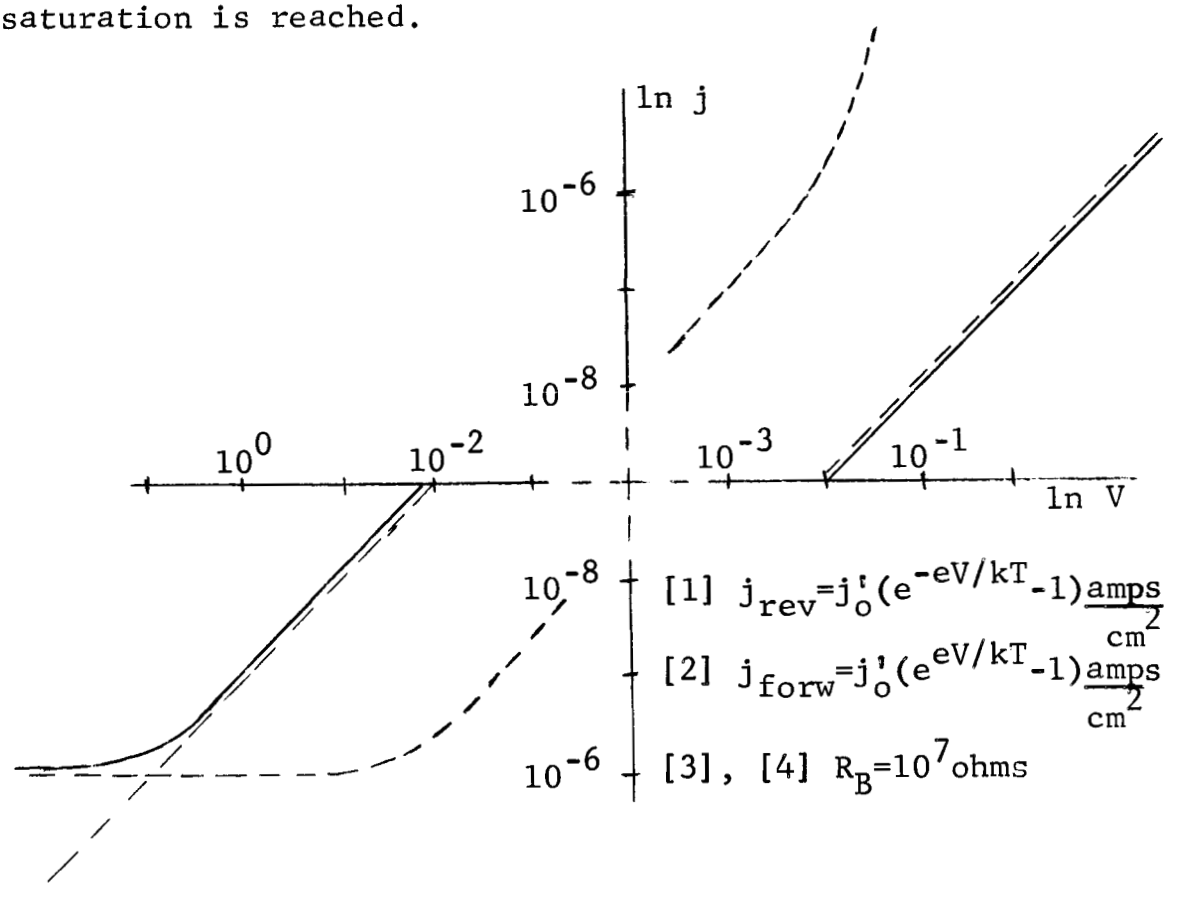

Graph (2). Solid line indicates I-V profile for $R_B=10^7$ohms and $j_o'=10^{-6}$ amp/cm^2.

For the case of a low bulk resistance (say $R_B = 10^3$ ohms) then the solid line in Graph (3) indicates the resulting I-V profile. Note that for the low bulk resistance the junction characteristic dominates in the reverse direction, and in the forward direction up to about 10^{-1} volts. At this point the I-V profile becomes bulk determined. (This particular choice of R_B and j_o' leads to rectifier-like characteristics of the junction - bulk semiconductor system).

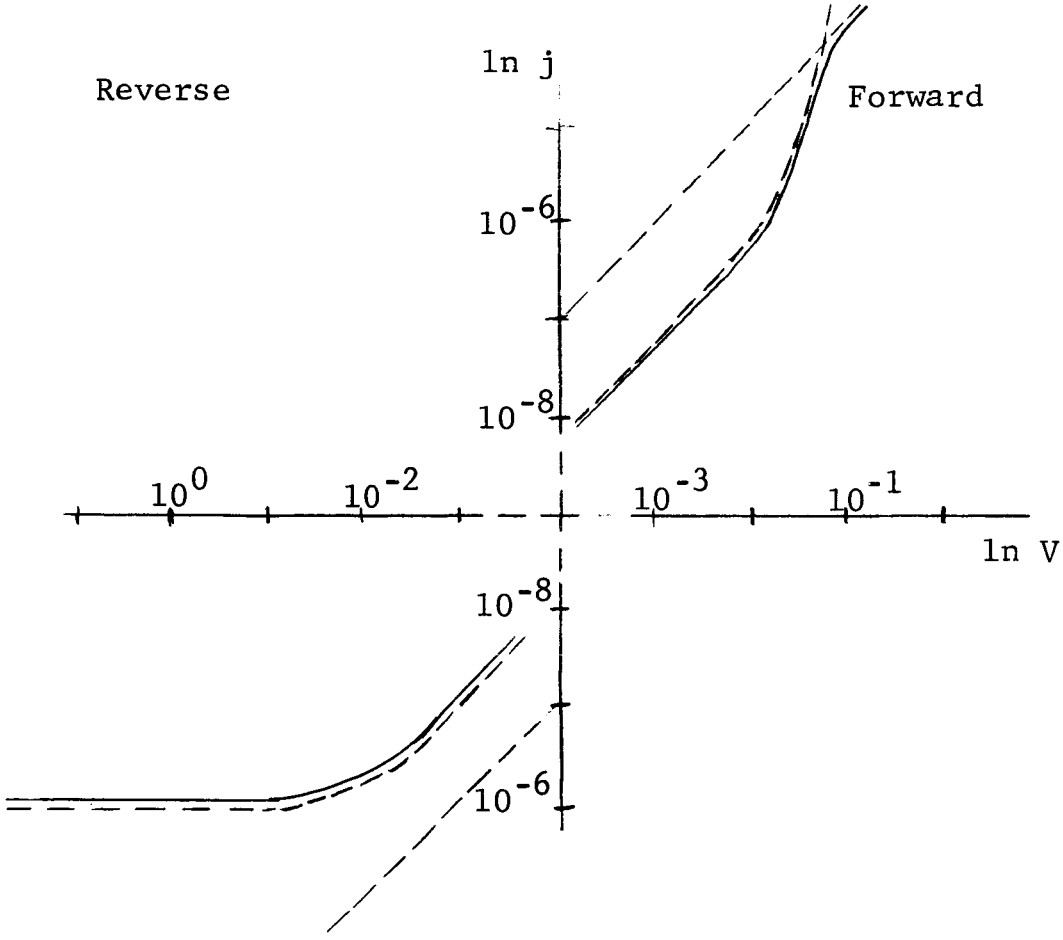

Graph (3). Solid line indicates I-V profile for $R_B=10^3$ ohms and $j_o'=10^{-6}$ amps/cm^2.

Before extending any further this type of graphic representation of junction characteristics, it is necessary to include the effect of field breakdown at the cathode (reverse biased junction). As it turns out, the width of the depletion layer for the blocking contact can be expressed using Poisson's equation:

$$\frac{d^2V}{dx^2} = \frac{eN_d^*}{K\epsilon_o} \tag{11}$$

where: N_d^* ≡ number of uncompensated ionized donors in the depletion region.

Integrating twice and using the boundary conditions that $\Phi=0$ at $x = o$, $\Phi = \Phi_m - \Phi_s$ at $x = w$, and $\frac{d\Phi}{dx} \simeq 0$ at $x = w$, gives the depletion layer width,

$$w = \sqrt{\frac{2K\epsilon_o[(\Phi_m-\Phi_s/e) + V_j]}{eN_D^*}} \tag{23}$$

where: V_j ≡ applied voltage at the junction.

Thus depending on the values of Φ_m, Φ_s, and N^*_d the width of the depletion layer can be (assuming $0.1 < \Phi_m - \Phi_s < 1.0$ eV. and $10^{13} < N_d^* < 10^{20}$ cm.$^{-3}$) from 10^{-7} to 10^{-4} centimeters. If now the I-V profile becomes dominated by the blocking contact such that essentially all the voltage, V_A, is applied at the depletion region, then a field of $V_A/(10^{-4}$ to $10^{-7})$ volts per centimeter exists at the barrier layer. Thus any time the I-V profile becomes determined by the reverse biased blocking junction, field breakdown will occur at the applied voltage $V_A = V_{br}$, or when $V_A = V_j/(10^{-4}$ to $10^{-7}) > 10^6$ volts/cm. What exactly happens at the junction after breakdown is not known except that the current depends on some fairly large power of the voltage.

The I-V profile in Graph (4) shows that in the case when $R_B = 10^5$ ohms there is a definite linear portion followed by the cathode saturation region. At voltages greater than

V_{br} the steep $j \propto V^n$ increase begins and continues until once again the current becomes determined by the ohmic resistance, R_B.

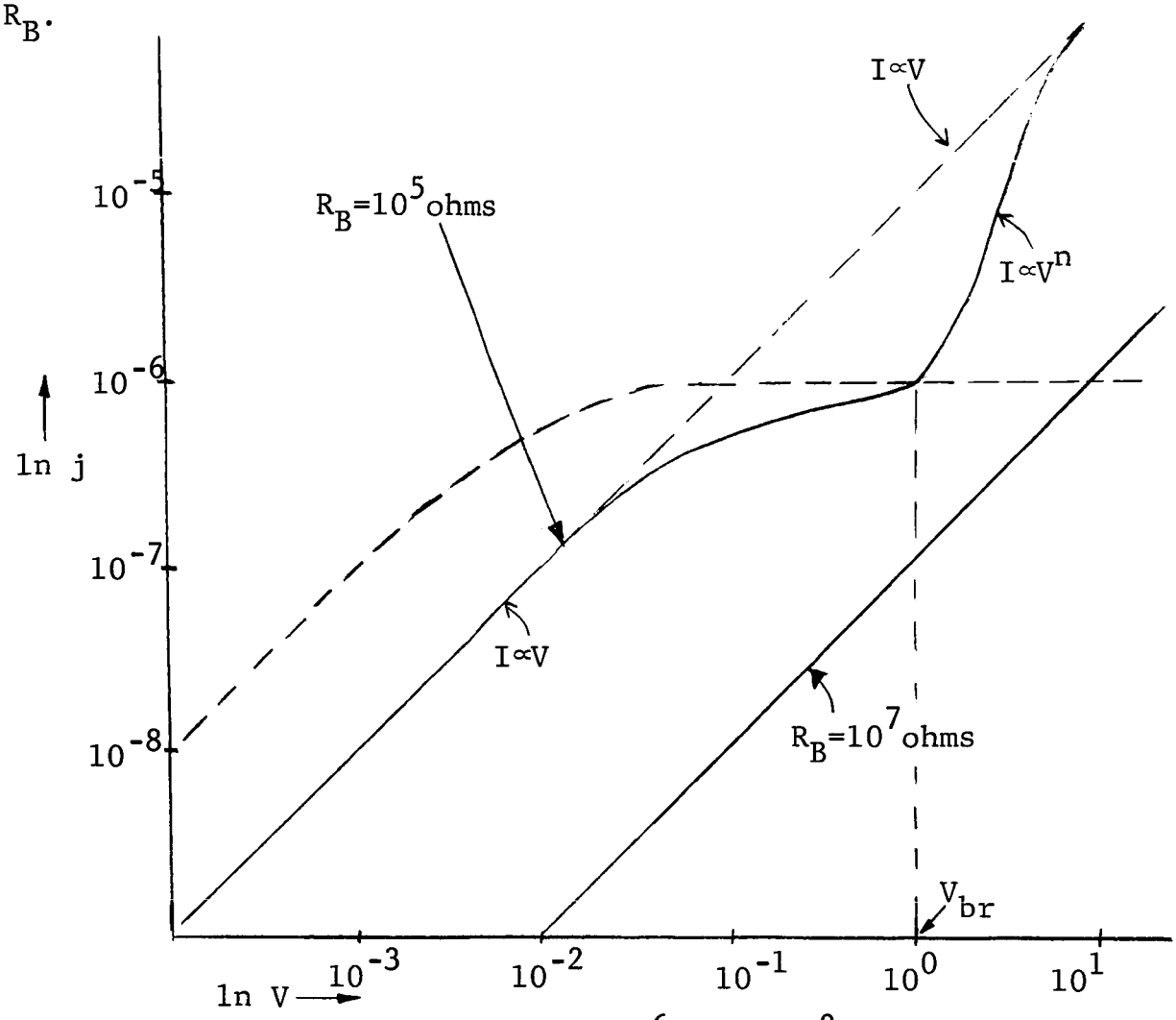

Graph (4). I-V profile for $j_o' = 10^{-6}$ amps/cm^2, assuming that barrier thickness is 10^{-6} cm, shown for cases when bulk resistance is 10^5 ohms and 10^7 ohms.

The I-V profile for $R_B = 10^7$ ohms in Graph (4) shows linearity for all voltages. However, the current saturation curve is crossed, but in this case the crossover point is at a voltage $10V_{br}$. Thus the barrier would breakdown almost without giving any indications in the I-V profile.

Solution to the current flow equation and the Poisson

equation for the case where $\Phi_s \geq \Phi_m$ yields, according to Mott and Gurney, $j \propto V^2$. In their development, however, the bulk crystal was already incorporated, therefore when constructing the I-V profile it is not necessary to plot a bulk resistance. The resulting I-V profile for the idealized injecting junction is shown in Graph (5).

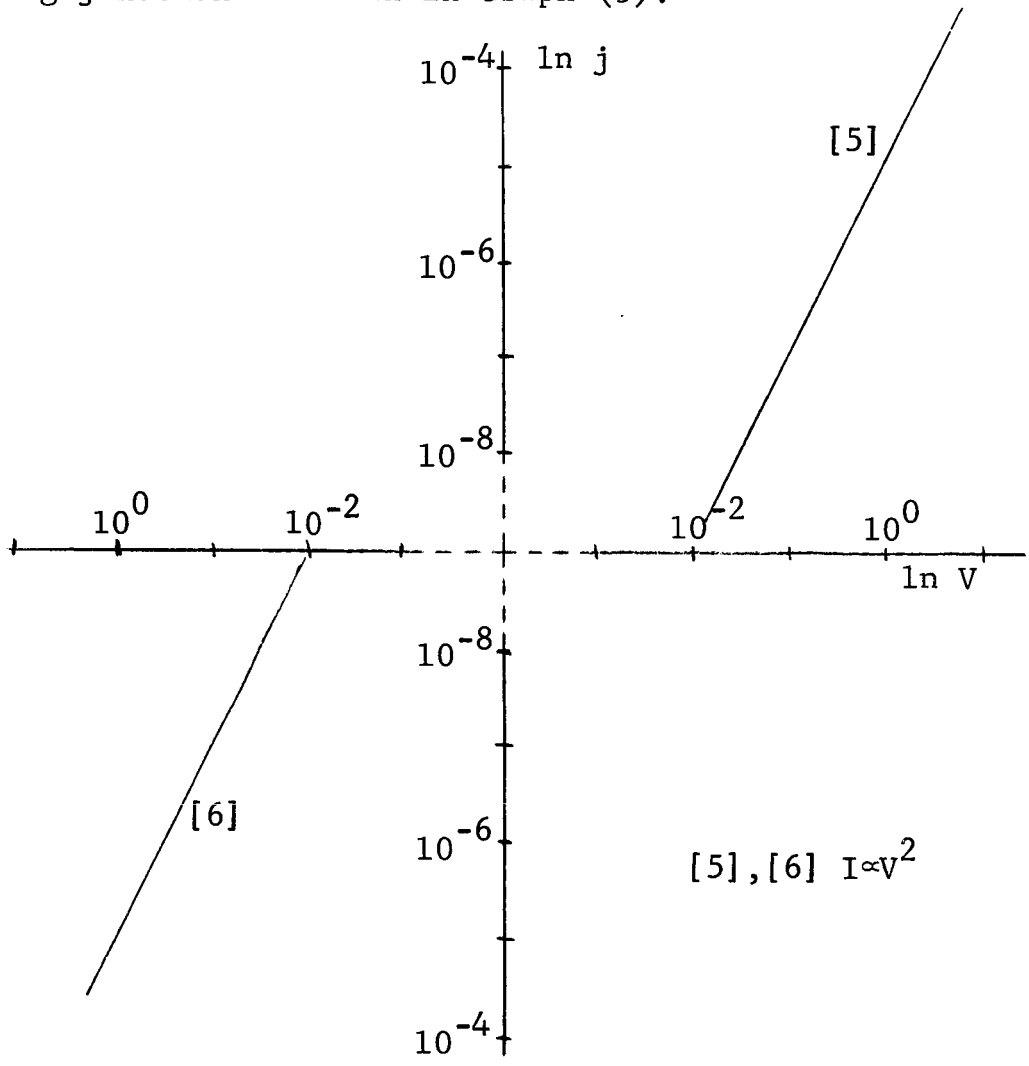

Graph (5). I-V profile for injecting contact, assuming no trapping effects in the bulk crystal.

In reality the existence of traps must be accounted for. Rose[3] took into account shallow traps, finding the trap-free equation to be reduced by a factor θ, such that

$$j = \frac{9}{8} \mu K \varepsilon_o \theta \frac{V^2}{d^3} \tag{24}$$

where θ represents the fraction of injected charge that remains free. If the number of traps is N_t at an energy, E_t, from the conduction band then

$$\theta = \frac{N_c}{N_t} e^{-(E_c - E_t)/kT} . \tag{25}$$

Lampert[4] developed a general theory for the injecting contact with traps in the bulk semiconductor. Lampert concluded that the I-V profile had to lie between three curves: $I \propto V^2$, $I \propto V$, and the trap filled limited curve. See Graph(6). At low applied voltages injection of excess charge is negligible, thus $I \propto V$. At increasing voltages charge is injected but trapped - hence $I \propto V^n$ $(1 \leq n)$. At a critical voltage, V_{TFL}, all traps are filled; then the I-V profile raises steeply and approaches the $I \propto V^2$.

In any event due to the small magnitude of the quantity $(\Phi_m - \chi)$, the injecting contact will probably not reach saturation - at least not within the power dissipation limits of the bulk crystal.

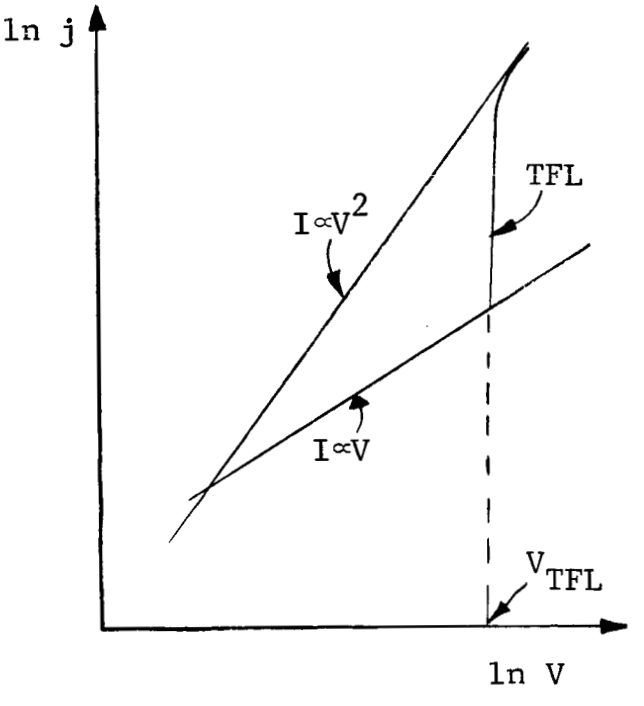

Graph (6). The "Lampert Triangle".

F. Junction - bulk crystal - junction I-V Characteristics. The next step is to consider the more realistic I-V profile of a junction - bulk - junction series circuit. Three cases will be considered: same contacts (both blocking) plus bulk, different contacts (both blocking) plus bulk, and one injection and one blocking contact plus bulk. (The case for two injecting contacts is essentially as was discussed for one injecting contact. This is so since an injection contact serving as an anode may be neglected as far as its significance on the space charge limited currents is concerned.)

1. For the two dissimilar blocking contacts the current is given as

$$j = \underbrace{\frac{V_{j1}}{R_{ji}}}_{j'_{rev.}} + \frac{V_B}{R_B} + \underbrace{\frac{V_{j2}}{R_{j2}}}_{j'_{forw.}} = \frac{V_A}{R_{j1} + R_B + R_{j2}} \qquad (26)$$

where:

$$R_{j1} = \frac{V_{j1}}{j'_{o1}(e^{-eV_{j1}/kt} - 1)} \qquad j'_{o1} = j'_{o2}$$

$$R_{j2} = \frac{V_{j2}}{j'_{o2}(e^{+\,eV_{j2}/kT} - 1)}$$

and

$$j = \frac{V_A}{\dfrac{V_{j1}}{j'_{o1}(e^{-eV_{j1}/kT} - 1)} + R_B + j'_{o1}(e^{+eV_{j2}/kT} - 1)}$$

The I-V profile is determined using equation (27). The case shown is for $R_B = 10^7$ ohms, $j_{o1} = 10^{-6}$ amps/cm^2. The profiles as drawn in the first and third quadrants of Graph (7) are identical. The resulting curve (solid line) gives a linear I$\propto$V Ohm's law type region that saturates at the

same current level and at the same voltage for either direction of current flow.

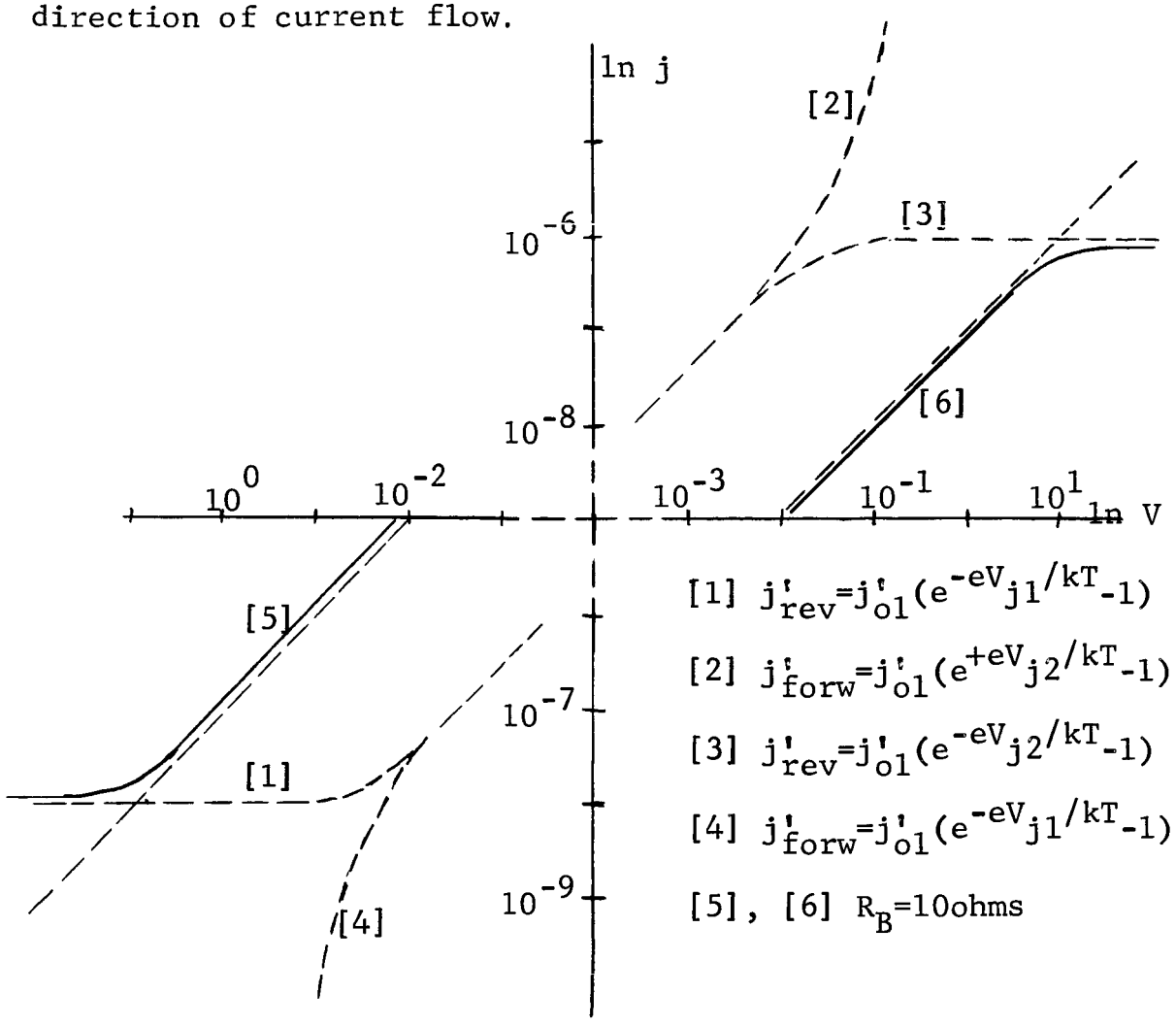

Graph (7). Solid line indicates I-V profile for "matching" junctions when $j_{o1}=j_{o2}=10^{-6}$ amps/cm^2 and $R_B=10^7$ohm.

For the case when $j_{o1} = j_{o2} = 10^{-6}$ amps/cm^2 and $R_B = 10^3$ ohms, the I-V profile takes on the character as indicated by the solid line in Graph (8). It can be seen that the I-V profile is the same for either direction of current flow. Considering for example quadrant I, the I-V current profile goes from a linear $I \propto V$ at low voltages (where $[e^{-eV/kT}-1] = 1 + \frac{eV}{kT} + \text{----} + (-1) \simeq \frac{eV}{kT}$), through a

transistion region, and then to a saturation region, $I = I_o$ (a constant) at high voltages. However, it can be noted that the linear part occurs for a much smaller range when the bulk resistance is smaller.

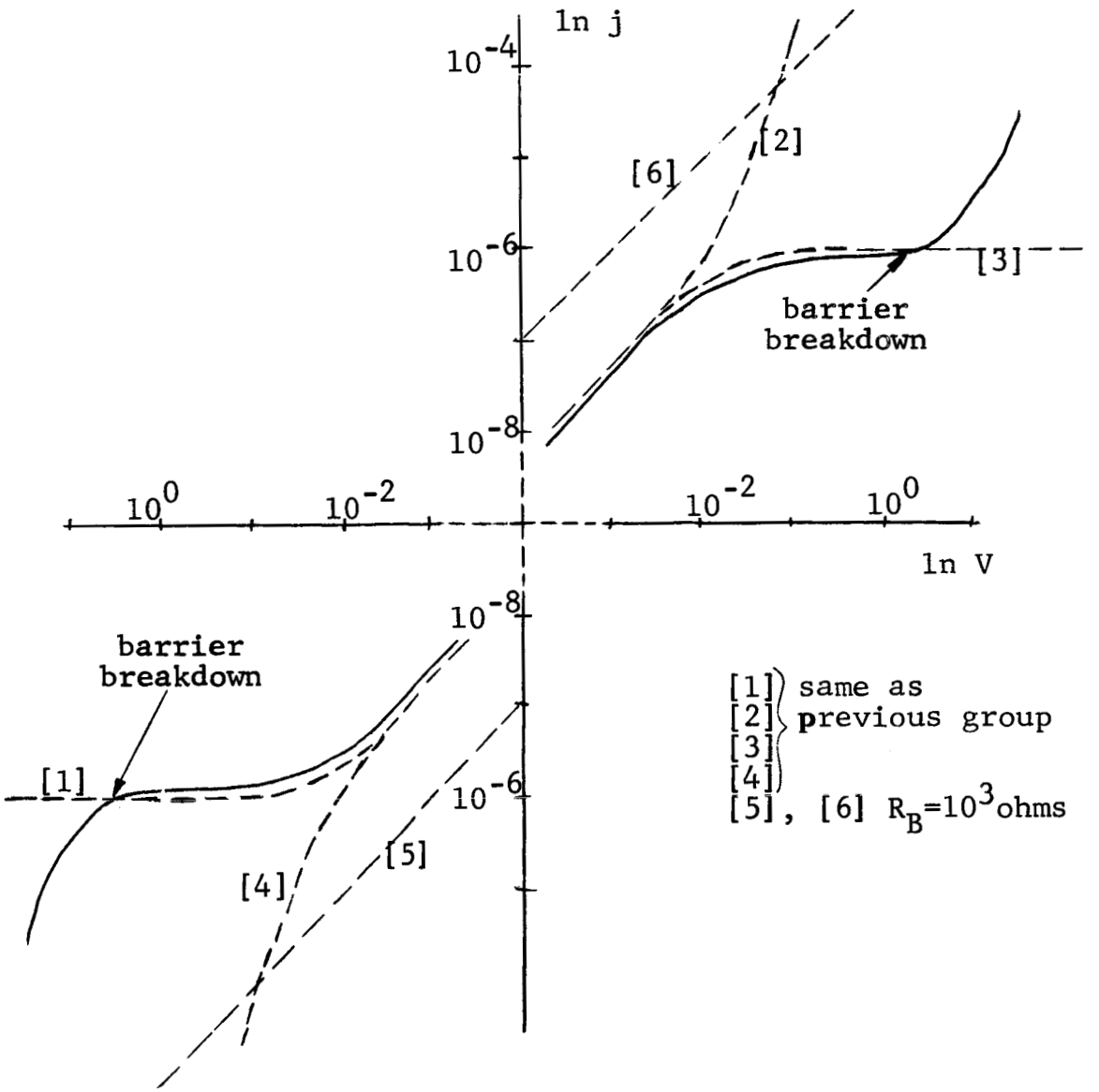

Graph (8). Solid line indicates the I-V profile for "matching" junction when $j'_{o1}=j'_{o2}=10^{-6}$ amps/cm^2 and $R_B=10^3$ohms. Note that barrier breakdown will probably occur if the barrier thickness is 10^{-5}-10^{-6}cm.

2. For two dissimilar contacts (i.e. one of say gold, the other of silver, such that the work functions of the two are different) equation (26) can be used to give I-V characteristics. It must be noted that this time

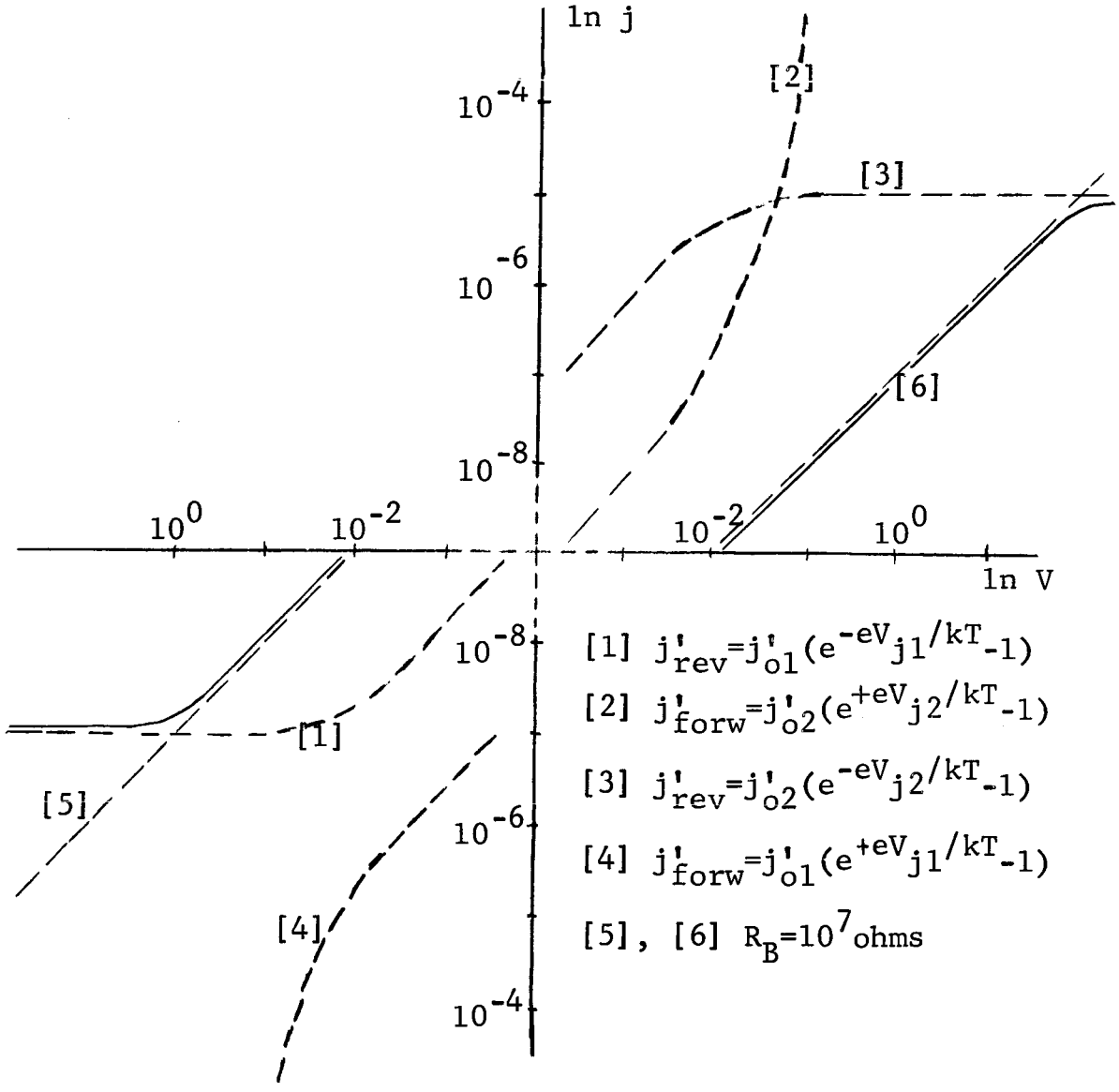

Graph (9). The dotted curves [1] and [4] represent, respectively, the case when the high work function junction ($j'_{o1}=10^{-7}$amps/cm^2) is reverse biased and the low work function ($j'_{o2}=10^{-5}$amps/cm^2) junction forward biased. Dotted curves [2] and [3] represent, respectively the high work function forward biased and the low work function junction reverse biased. The solid line represents the I-V profile when the bulk resistance is 10^7ohms.

$j_{o1} \neq j_{o2}$ (i.e. $\Phi_{m2} \neq \Phi_{m1}$) such that

$$j = \frac{V_A}{\frac{V_{j1}}{j'_{o1}\,(e^{-eV_{j1}/kT}-1)} + R_B + \frac{V_{j2}}{j'_{o2}\,(e^{+eV_{j2}/kT}-1)}} \qquad (28)$$

and $j_{o2} > j_{o1}$ or $\Phi_{m2} < \Phi_{m1}$.

Graph (9) shows, using equation (28), the case for $j_{o1} = 10^{-7}$amps/cm^2, $j_{o2} = 10^{-5}$amps/cm^2 and $R_B = 10^7$ohms. Note that the resulting I-V profile is linear for awhile in both directions. For one direction the saturation occurs at a higher current value than for the other direction; this is because of the difference of the work functions of the metals at the two junctions.

Graph (10) describes the case of low bulk resistance ($R_B = 10^3$ ohms) and dissimilar junctions. Note that the resulting I-V profile shows rectification effects; the rectification ratio at high voltages (above 1 volt for the case described) being that of the two saturation currents j_{o1} and j_{o2}. Greater rectification ratios can be obtained by choosing the electrode metals such that the work functions are quite different. Also for this case, the resultant profile is almost the same as a single junction and bulk in series. In the reverse biased case (i.e. low work function metal positive) the current saturates almost immediately. In the forward case (i.e. low work function metal negative) the current increases exponentially with the applied voltage at the high work function junction. At higher voltages ($>10^{-1}$ volts in this particular example) the lower work function junction saturates and in so doing dominates the I-V profile.

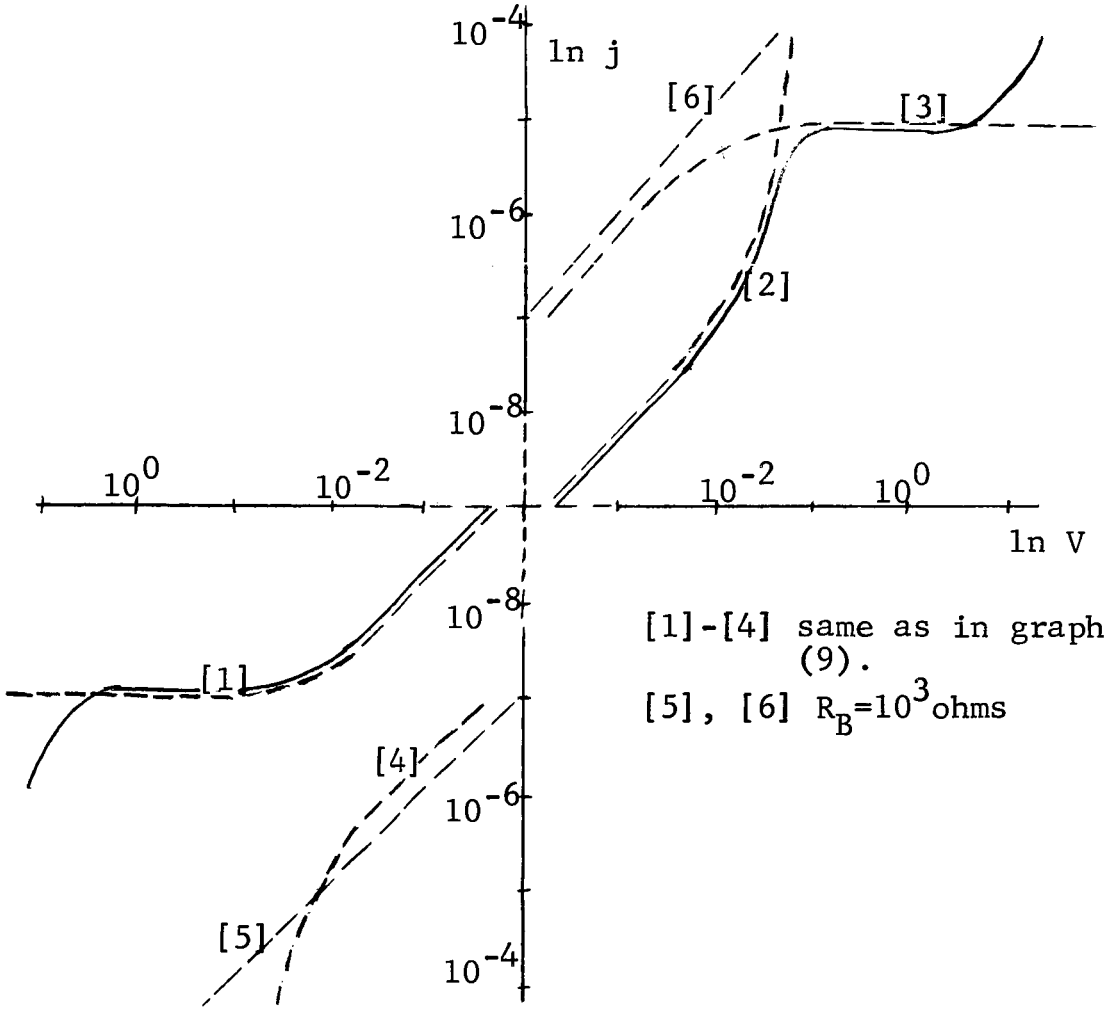

Graph (10). Solid line indicates the I-V profile for case when $j_{o1}=10^{-7}$ amps/cm^2, $j_{o2}=10^{-5}$ amps/cm^2 and $R_B=10^3$ohms. (Note the deviation from current saturation when barrier breakdown occurs).

3. The case of one injecting and one blocking contact plus bulk (see Graph 11) yields the rectification effect as described previously. In the reverse biased orientation (blocking contact metal negative, injecting contact metal positive) the current saturates as determined by the blocking contact junction. In the forward biased orientation (blocking contact metal positive, injecting contact metal negative) the curve at low voltages may (depending on the trapping that occurs) increase exponentially as the voltage at the blocking contact. At higher voltages the

theoretical Mott and Gurney square law dependence is expected.

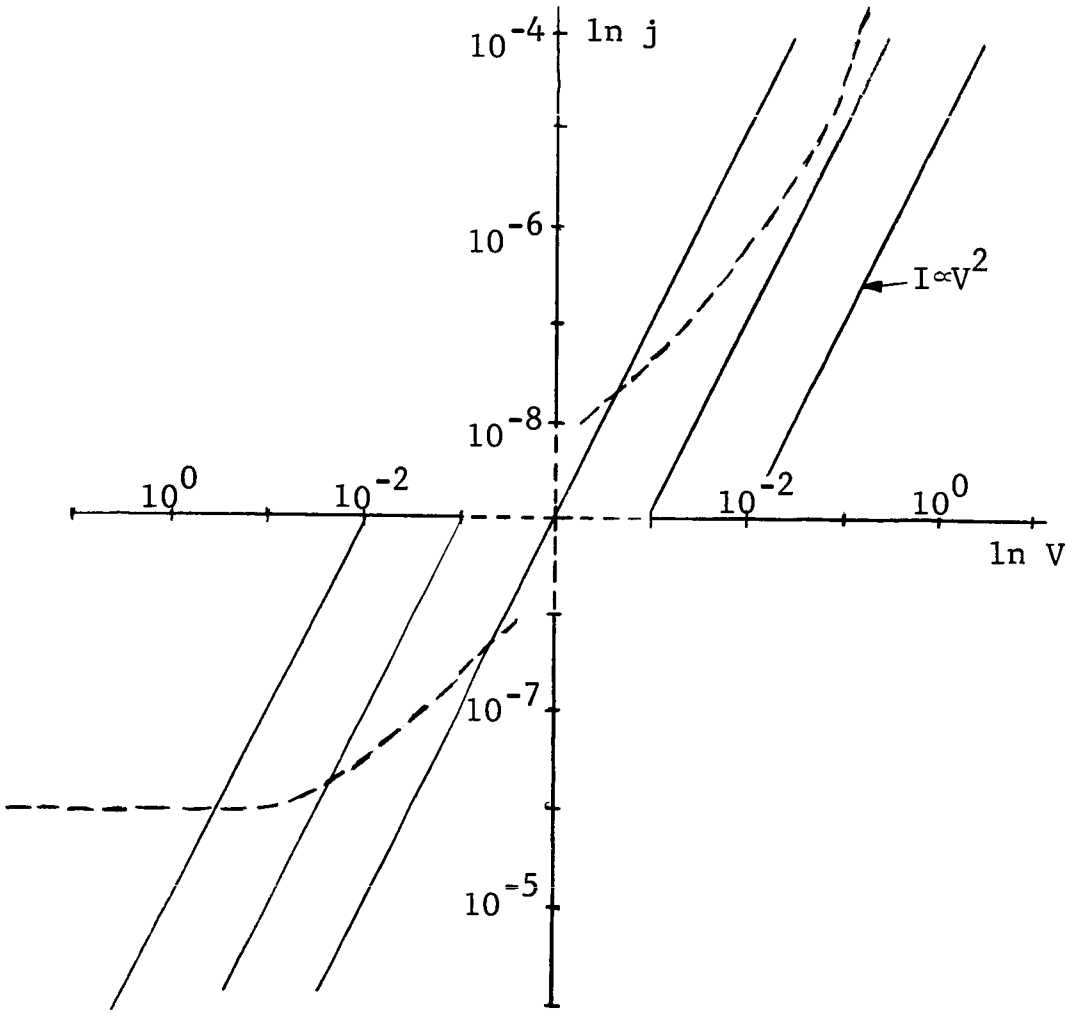

Graph (11). Solid line represents I-V profile for case one blocking junction ($j_o'=10^{-6}$ amps/cm^2) as done in junction contact. The series of $I \propto V^2$ curves represents SCLC for different values of θ.

In conclusion it can be seen that a high resistance bulk (10^7 ohms in the examples cited above) effects the junction - bulk and junction - bulk - junction circuits in such a way as to permit the I-V profile to have a linear region at low applied voltages which extends above the linear kT equivalent voltage range (i.e. where $e^{-eV/kT}-1 \simeq \frac{eV}{kT}$). When in the same circuit the bulk resistance is small (10^3 ohms in the examples cited above), the I-V

profile is almost fully determined by the junction up until the time when the breakdown voltage at the barrier is reached.

In the CdS-metal junction,the CdS, which is the bulk resistance, can experimentally be varied since it is photosensitive. Thus it should be possible to observe both linear and bulk determined I-V curves as well as junction determined curves by changing the light intensity. This is indeed the case as was demonstrated by Ruppel[5]. His family of curves, however, also tended to saturate at higher current levels for high light intensities. This would correspond to a lowering of the barrier or resistance at the junction which could quite conceivably also be light dependent.

III. EXPERIMENTAL CONSIDERATIONS

A. Previous Work. In trying to experimentally achieve an ohmic contact to CdS (i.e. a low electrical resistance contact which acts as a reservoir for electrons) there has been done an extensive amount of work. From considering the simplified junction model, the obvious choice would be metals which have a lower work function than the work function that would reasonably exist on cadmium sulfide.[b] For CdS this kind of approach leads to a choice of In, Ga and possibly Al as having the property of $\Phi_m < \Phi_s$. This approach, it must be emphasized, can only serve to indicate possible choices of a metal to serve as efficiently performing electrical contacts. The factors of surface states, surface contamination, and change in properties of the two systems when they are brought into intimate contact, all play a crucial part in the experimentally observed contact.

Initial attempts to create ohmic contacts include the approach of Butler and Muscheid[6] who found that treatment of the CdS crystals with a low pressure gas discharge before application of the contact yielded ohmic behaving electrodes-even for metals for which by work function considerations should not have worked. However, the ohmic behavior effects disappeared with heat treatment at 200°C or for extended periods of time. This occurence was explained by Fassbender[7] who reasoned that the initial gas discharge created donor levels on the surface of the crystal. However, with time-or

---

[b] It must be remembered that the work function in a semiconductor, because of its definition in terms of the Fermi level, varies significantly with degree of impurity concentration and temperature.

heating-the donor levels would anneal out and what had been ohmic contacts became current-determining-blocking contacts.

Smith[8] demonstrated by various measuring techniques that In and Ga did make ohmic behaving contacts to CdS as was predicted by consideration of the simplified junction theory. Also, in agreement with the simplified theory, it was found that such metals as Au, Cu, Ag, and Pt, which have larger work functions than the work function for strongly n-type CdS, exhibited blocking contact behavior.[9, 10]

Sihvonen and Boyd[11] investigated contact characteristics for ten metals which work function-wise bracketed cadmium sulfide. They used one evaporated In plate contact and one point contact, being made of the particular metal being investigated. They found that by passing a moderately intense electric current pulse, the point contact, which was previously characterized by blocking behavior and exhibiting diodic performance, became ohmic. They reasoned that the current pulse punctured the depletion barrier, which permitted electrons to tunnel more freely and in greater numbers.

The work done by Böer and Lubitz[12] substantiated earlier findings concerning the behavior of various metals as contacts using the method of evaporation. They found that heating the CdS crystal before evaporating on the electrode increased the chances for attaining ohmic behaving electrodes. Heating of the CdS crystal while in the vacuum desorbed some of the physically adsorbed impurity layers (oxygen, nitrogen, etc.) that existed on the CdS surface. They cited the difficulty of using indium as electrodes to CdS at high temperature ($>100^{o}C$), since at these temperatures, massive diffusion of the indium occurs. The diffused indium acts as a donor[13] which, of course, may mask the other characteristics of the crystal.

Boer and Lubitz felt Al would serve ohmically on CdS. The

subsequent experiments showed that this indeed was true, in about 50% of the investigations, but only if the CdS crystals were heat treated in a very high vacuum before the aluminum electrode was deposited. It was also determined that further heat treatment of the aluminum on the CdS crystal did not result in any detectable diffusion of aluminum into the crystal up to 350°C.

Spitzer and Mead[14] studied contact behavior in terms of barrier heights. Generally, they found that metals having work functions greater than CdS were blocking, while those with work function less than CdS were injecting or neutral. They prepared their contacts by "vacuum cleaving" the CdS crystal before depositing by evaporation the metal to be used as the electrode. This procedure enabled studies to be made for metal-semiconductor junctions which were as intimate as possible, in that by cleaving the crystal, a relatively pure CdS surface would exist for the deposition of the electrode film.

B. A New Approach. Unfortunately, none of the above procedures (with the possible exception of Böer and Lubitz's partial success with aluminum) permit treatment of the entire junction system at temperatures >100°C without there being significant electrode diffusion into the CdS or destruction of the ohmicity of the contact. The method of Boyd and Sihvonen permit use of other metals besides In to be used as ohmic contacts, but the electrode configuration (one point contact, one plate contact) is unwieldly. It becomes difficult to interpret data with any accuracy because of the complicated electric field that would exist between a point and a plate. Thus, further investigation into the problem of creating "heat resistent ohmic contacts" (HROC)[c] to cadmium sulfide seems desirable.

---

[c] The expression heat resistant ohmic contact (HROC) is used to denote a contact which remains ohmic when heated up to at least 300°C.

As indicated by Böer and Lubitz and substantiated by Goodman[15] the difficulty with using aluminum is the existence of an interfacial layer between the aluminum and the cadmium sulfide. It is a fair assumption to say that the component of the interfacial which causes the problems is oxygen. Because aluminum has such a high affinity for oxygen, it will react with any oxygen impurities present on the CdS surface. It is well known that aluminum oxide is an excellent insulator, thus its presence on the surface of CdS will create non-ohmic behavior. However, the fact that aluminum can serve as a good ohmic contact was effectively demonstrated by Spitzer and Mead[14] who evaporated metals onto vacuum cleaved CdS crystals.

It was with this view in mind that Böer[16] suggested a multilayer technique wherein aluminum and indium could serve as HROCs to CdS single crystals. This electroding technique called for an evaporation in vacuum of a monolayer of a preparative metal, followed by several layers of an active metal and finally many layers of a covering metal. The purpose of the preparative metal was to enhance impurity desorption from the cadmium sulfide surface; the active metal would act as the ohmic behaving electrical contact to the bulk. The covering metal would serve not only as a means by which current can be carried to the bulk via the active metal, but also as a sink for any excess active metal which might diffuse.

The initial choice was to use indium or aluminum as the active metal, and gold as the covering metal. When aluminum was used, the gold was also to function as the preparative metal since it was felt that gold would sufficiently enhance impurity desorption from the CdS surface by the physical mechanism of collision. After the crystal surface had been "cleaned" in this manner, it would be possible to have relatively intimate contact between the

aluminum layers and the CdS; such a CdS-aluminum contact should then perform ohmically. In the case of indium, it was reasoned that if only a monolayer of the indium was deposited, it could be trapped at the CdS surface and thus might not readily diffuse into the bulk.

As a result of a suggestion to Böer by Diemer, titanium was used as the preparative metal in the multi-layer technique. Since titanium has a stronger affinity for oxygen than aluminum, deposit of a monolayer of titanium would enhance a "pseudo-desorption" of oxygen from the surface by a chemical reaction mechanism that reduces the aluminum oxide and forms a titanium oxide. Thus, an aluminum layer will have the opportunity to make relatively intimate contact with the "pure" CdS. The benefit of this choice of electrode material would continue even after the initial evaporation. For if aluminum oxide were to form in some manner, the excess Ti existing on top of the initial layers of Al and Ti would serve to reduce the aluminum oxide by

$$2Al_2O_3 + 3Ti \rightarrow 3TiO_2 + 4Al \,. \tag{29}$$

The other consideration in experimentally creating the electrical contacts using the multi-layer technique was the vacuum environment. High vacuum conditions alone will not substantially correct the situation by ridding the surface of oxygen, but they will prevent further oxidation from occuring during evaporation of the electrode material. This result turns out as a consequence of considering kinetic theory. In kinetic theory, the number of gas molecules at a pressure, P, and absolute temperature, T, striking the unit area of a plane surface in unit time is given by:

$$N = \frac{P}{(2\pi mkT)^{1/2}} \,. \tag{30}$$

Thus, for an oxygen pressure of 10^{-5}mm. Hg at room temperature, N = 5.2×10^{15} at. cm^{-2} $sec.^{-1}$. Then taking the area occupied by a single adsorbed atom of oxygen on the surface to be 1.4Å^2, it is seen that at this pressure of oxygen the rate at which the residual atoms strike the target is such as to form a monolayer in about one second. Since the rate of deposition of the electrode metal is large compared with that for the condensing oxygen under evaporation conditions, in order to avoid interference by residual gas, the evaporation must be carried out at pressure much lower than 10^{-5}mm.[17] In other words, if the deposit of a monolayer of titanium takes 5 seconds and the oxygen pressure is 10^{-5}mm., then there would be sufficient time for another oxygen layer to form on top of the Ti layer.

With the above consideration in mind, evaporation of the metal electrodes was hopefully to be performed at pressures less than 10^{-6}mm. An additional effort was made to reduce the oxygen partial pressure by flushing the vacuum system with nitrogen or argon before vacuum take down.

IV. APPARATUS AND PROCEDURE

A. Preparing the contacts. The crystals chosen for contact study were supposedly non-doped. The photosensitivity varied from crystal to crystal, as did their dark currents. There was no quantitative effort to determine any electrical characteristics on the crystals that were to be electroded.

It must be emphasized that the whole experimental procedure of electroding the CdS crystals was carried out with utmost cleanliness. Neither the crystals nor any interior element of the vacuum system in which the electroding took place were touched with ungloved hands.

The crystals to be electroded were placed in the crystal holder as shown in Figure (5). The crystal was held in place by a mask of aluminum foil which was larger in area than the crystal.

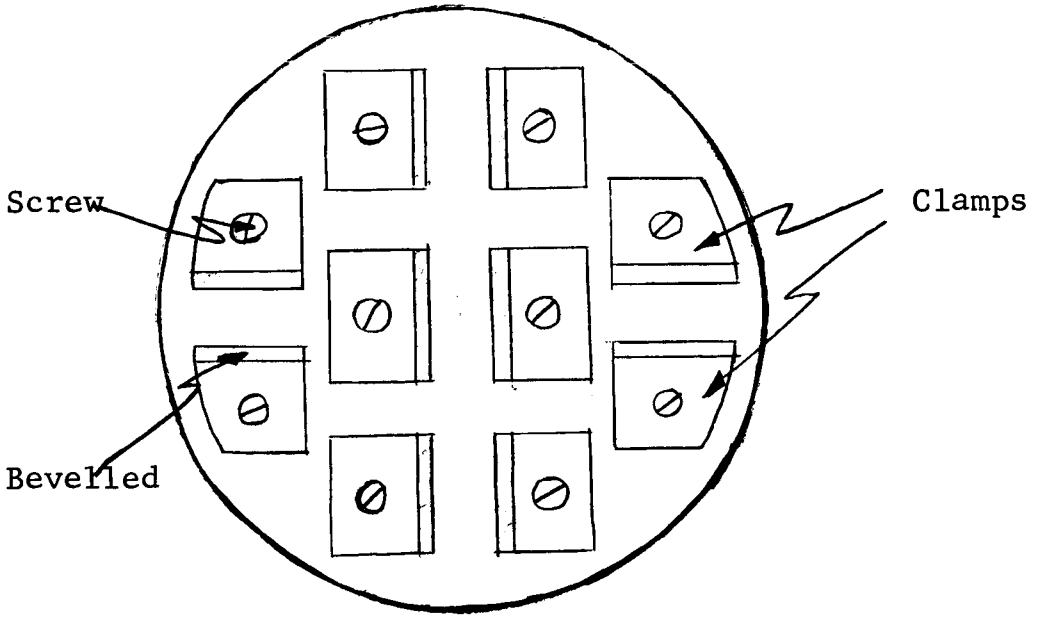

Figure (5). The crystal holder.

The overhang of the masking foil was clamped to the crystal holder as shown in Figure (6). An opening was cut in the foil to allow the evaporated material to reach the crystal. A metal strip .7mm wide was used to create two separate electrodes each being approximately 10^{-1} cm.^{2}.

SIDE VIEW

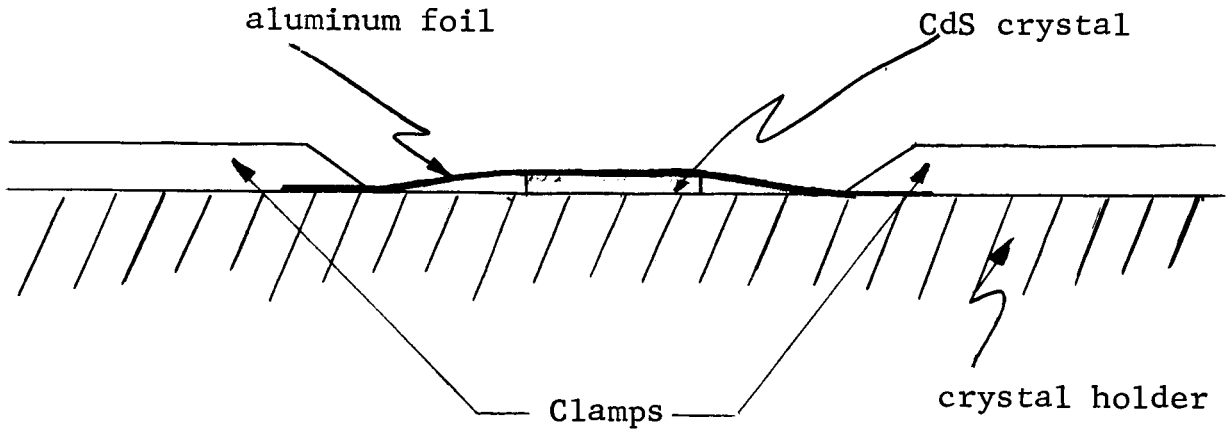

TOP VIEW

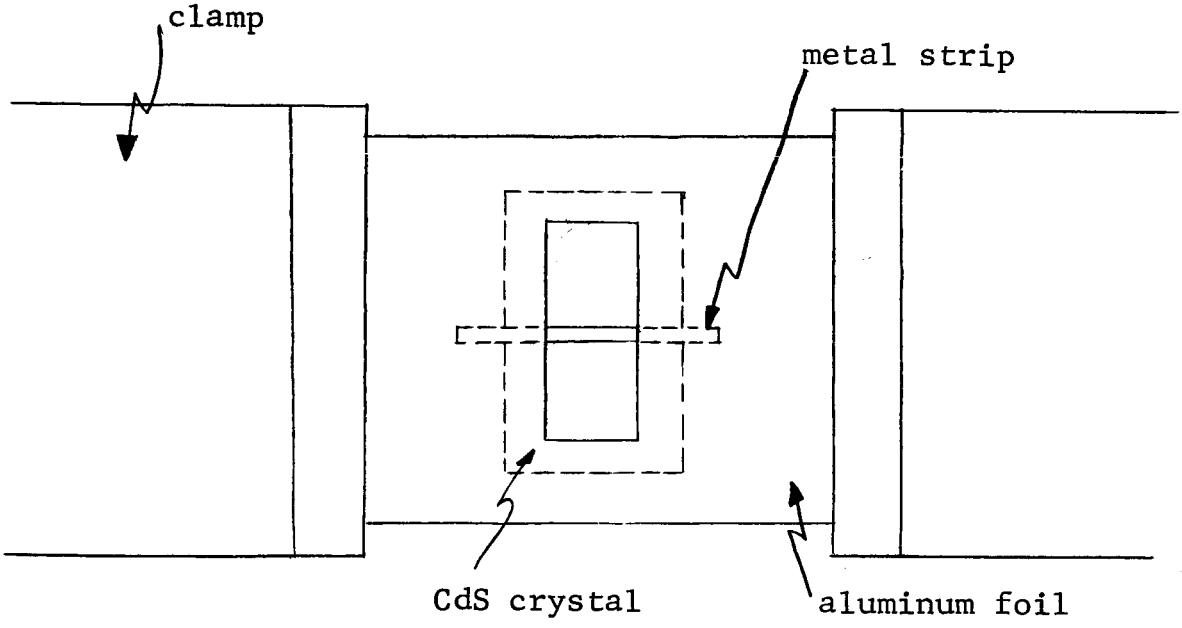

Figure (6). Top and side view of crystal as it is positioned on the crystal holder.

The crystal holder with the crystals mounted was placed in the bell jar of a diffusion pump vacuum system as shown in Figure (7). A model 1415 Welsh mechanical pump was used with Dow Corning 704 oil. Cold trap #1 between the forepump and the diffusion pump, which used liquid nitrogen as a coolant, avoided backstreaming of the forepump oil into the high vacuum side. The diffusion pump was the Heraeus with a four inch throat using Dow Corning 705 oil. Cold trap #2 between the diffusion pump and the bell jar minimized oil

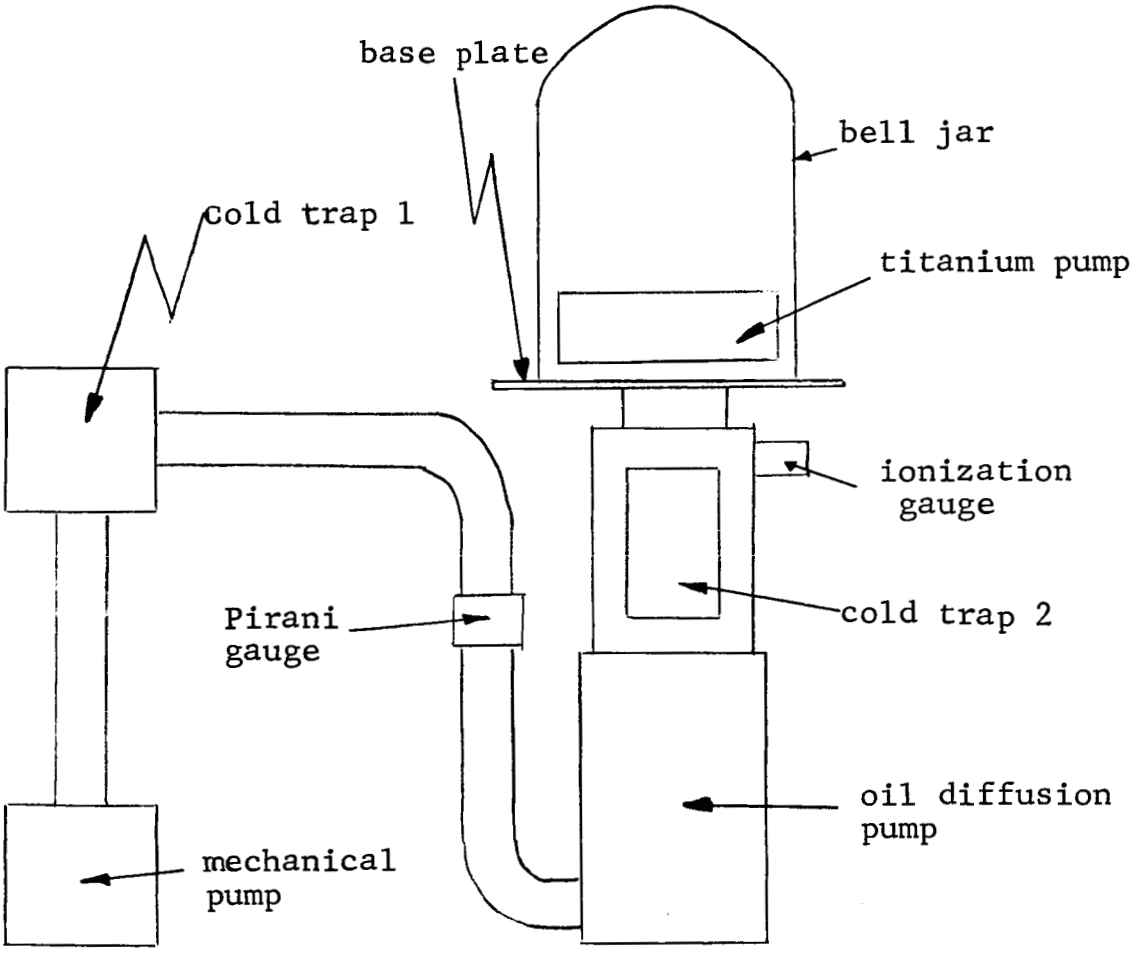

Figure (7). Schematic of the vacuum system in which electrodes were evaporated onto the CdS crystals.

backstreaming and also functioned as a cryogenic pump. Also incorporated in the system was a titanium sublimation pump which used a Varian titanium filament that had been wrapped with additional windings of tungsten to give better sublimation rates and longer filament lifetime.

Two gauges were used to measure the system pressure. A CVC Pirani Gauge type GP 110 was used to measure the high pressure side; this pressure stayed below 5 microns after the initial takedown. A Varian ionization gauge and control unit (model 971-0003) was used to determine the low pressure side; this bell jar system was always less than 5×10^{-7} mm prior to evaporation.

Figure (8) shows schematically the configuration of the various components in the bell jar system. Each high

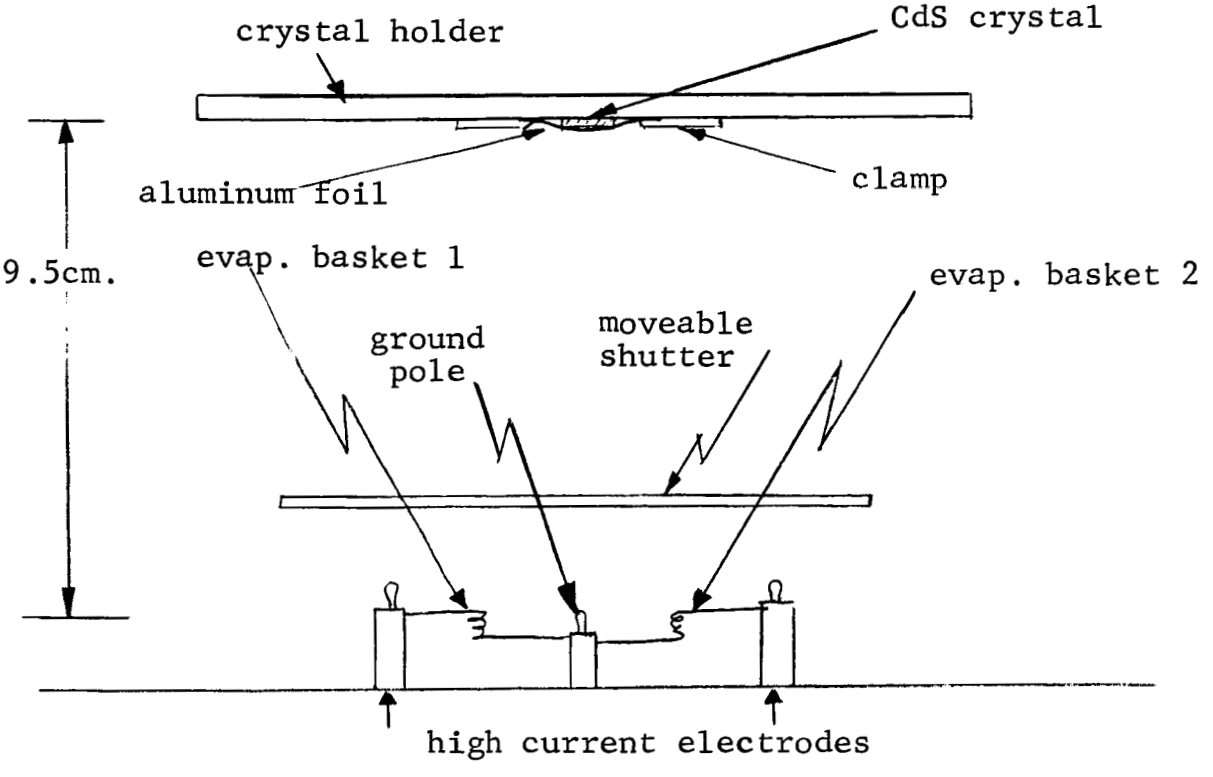

Figure (8). Schematic of components used for evaporation.

current electrode was connected to a tungsten evaporation basket containing the various electrode metals and was regulated by a separate control unit. Over the two baskets there was a magnetically controlled movable shutter which, when positioned correctly, prevented a direct optical path from either basket to the crystal holder. At a distance of 9.5 cm. from the baskets, the crystal holder was positioned. Finally, in an attempt to determine the effect of various ambient gases on electrode performance, the bell jar system was flushed with nitrogen, argon, or oxygen before the evaporation was begun.

During the system take down the contents of the evaporation baskets were outgassed. To make sure none of the basket contents reached the CdS substrates during outgassing, this procedure was done using the movable shutter. When the evaporation was to be performed, both baskets were fired such that the contents of the baskets were initially depositing layers on the movable shutter. Then the shutter was moved so that there was a deposition on the CdS substrate only from the basket containing the preparative metal. After a predetermined time the shutter was moved from its position over the basket containing the active metal, and its contents were deposited simultaneously with the preparative metal on the CdS substrate. The procedure was terminated by depositing several layers of a covering metal. During the course of the evaporation the pressure in the bell jar system steadily increased reaching a peak which was dependent on the metal being evaporated. This peak pressure, however, never went above 6×10^{-6} torr.

B. Measuring the Contact Properties. The electroded crystal to be investigated was placed on the cryrostat table as shown in Figure (9). The table and a "heat" cover which was used to maintain stabilized temperatures at the

crystal, were placed in the cryrostat system. This system

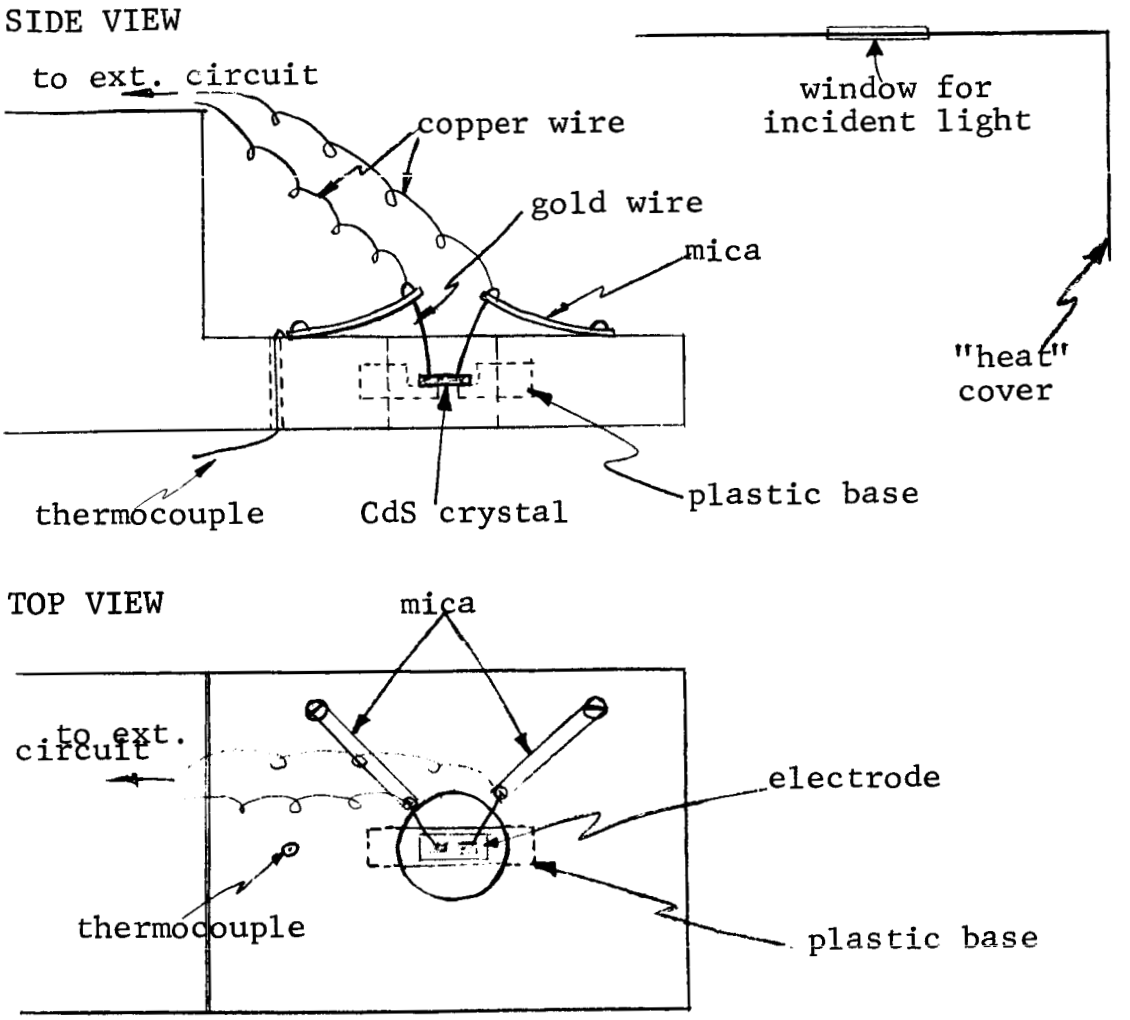

Figure (9). Schematic of cryrostat table and "heat" cover.

could be evacuated to a pressure of 10^{-2} torr and was equipped such that the cryrostat temperature could be varied over the range from -190°C to 300°C.

The method of investigating contact properties was low frequency noise measurements and current versus voltage

curves (henceforth called I-V curves). At the low frequency end of the noise spectrum of CdS, there is a large component of noise that increases as 1/f. As the electrical character of the contacts improve, this component of the noise decreases. A more extensive treatment of the theoretical aspects of this phenomenon can be found in the work of MacFarlane.[18] The method of using I-V curves to determine junction properties follows from the discussion in Chapter II.

A schematic of the entire system used for the measurement of I-V curves is shown in Figure (10). A unitron light source operated at 4 volts, giving a color temperature of 2520°K, was used in conjunction with a 517 mμ band pass filter (half-width 190Å) to uniformly irradiate the CdS crystal. The light intensity, I_o, was calculated for the optical set-up and was found to excite, assuming a quantum efficiency of one, about 6×10^{16} electrons/cm^3 sec. A series of Kodak grey filters were available to vary the intensity of the irradiating light by as little as a tenth of an order of magnitude.

Figure (11) show the electrical circuit used for the I-V measurements. A voltage divider used in conjunction with a Heathkit power supply applied a voltage in the range from 1 mv. to 400 volts to the crystal. The current through the crystal was detected by a Keithley 417 linear micro-micro ammeter. Because of grounding requirements it was necessary to use two electrometers, attaching one to each electrode.

A schematic for the noise measurements is shown in Figure (12). Since the amplitude of the contact noise was so low and would be distorted by the presence of an a.c., it was necessary to eliminate all components using a.c. Thus a separate voltage supply and light source that did not

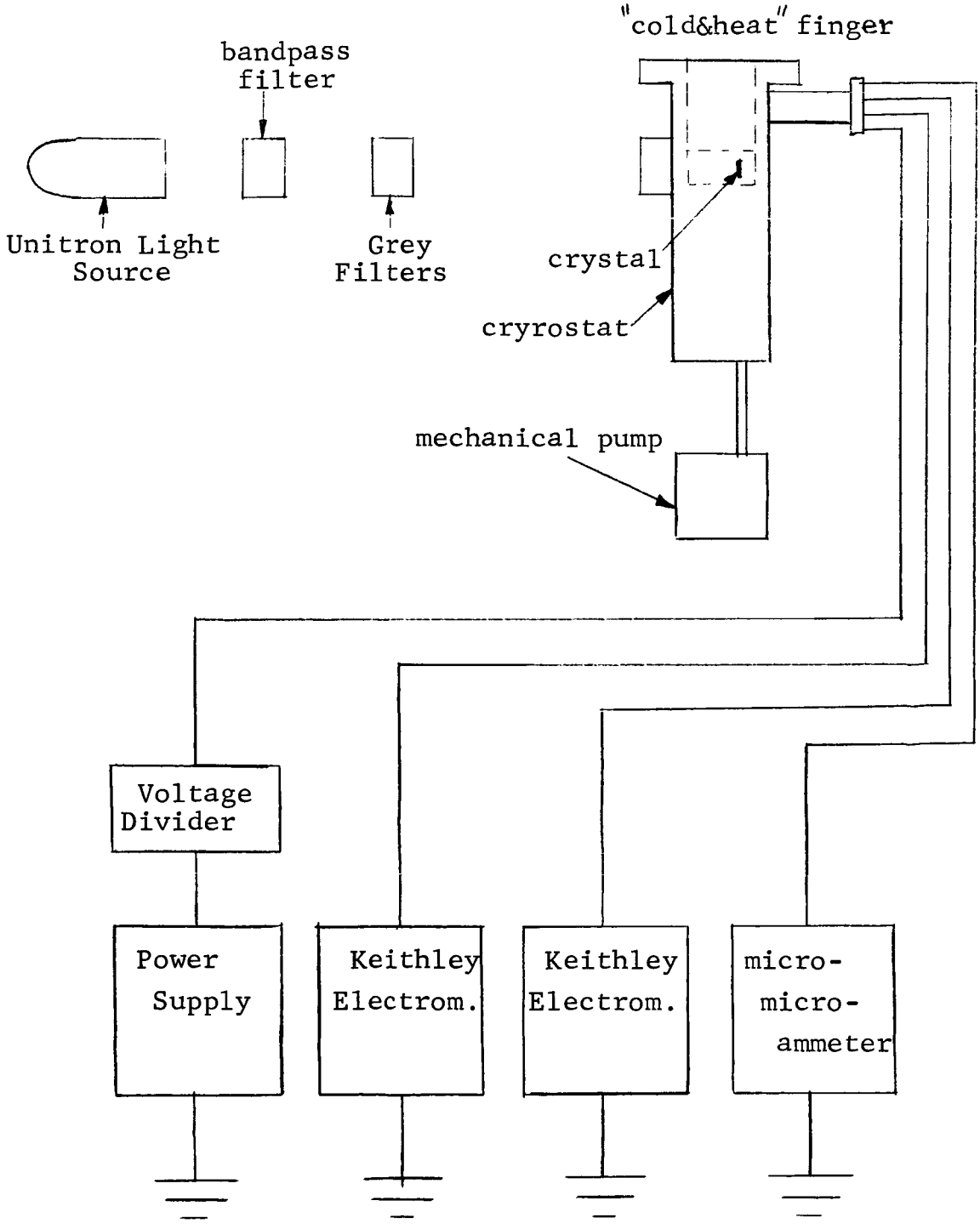

Figure (10). Schematic of apparatus used to measure I-V curves.

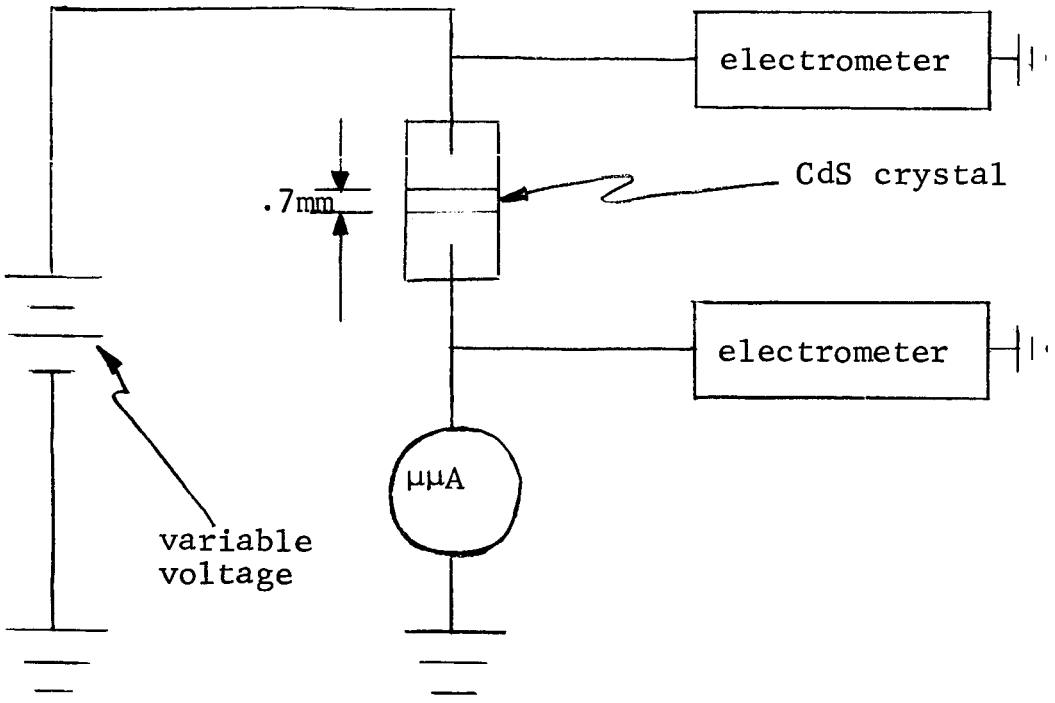

Figure (11). Electrical circuit used in I-V measurements.

utilize a.c. were incorporated into the circuit. A variable resistance box, which was in series with the crystal, was used in conjunction with the Keithley amplifier - frequency selector and a Tektronix Type 543A oscilliscope. Two frequency ranges, 10 - 100cps and 100 - 300cps, were selected for the calculation of the 1/f noise.

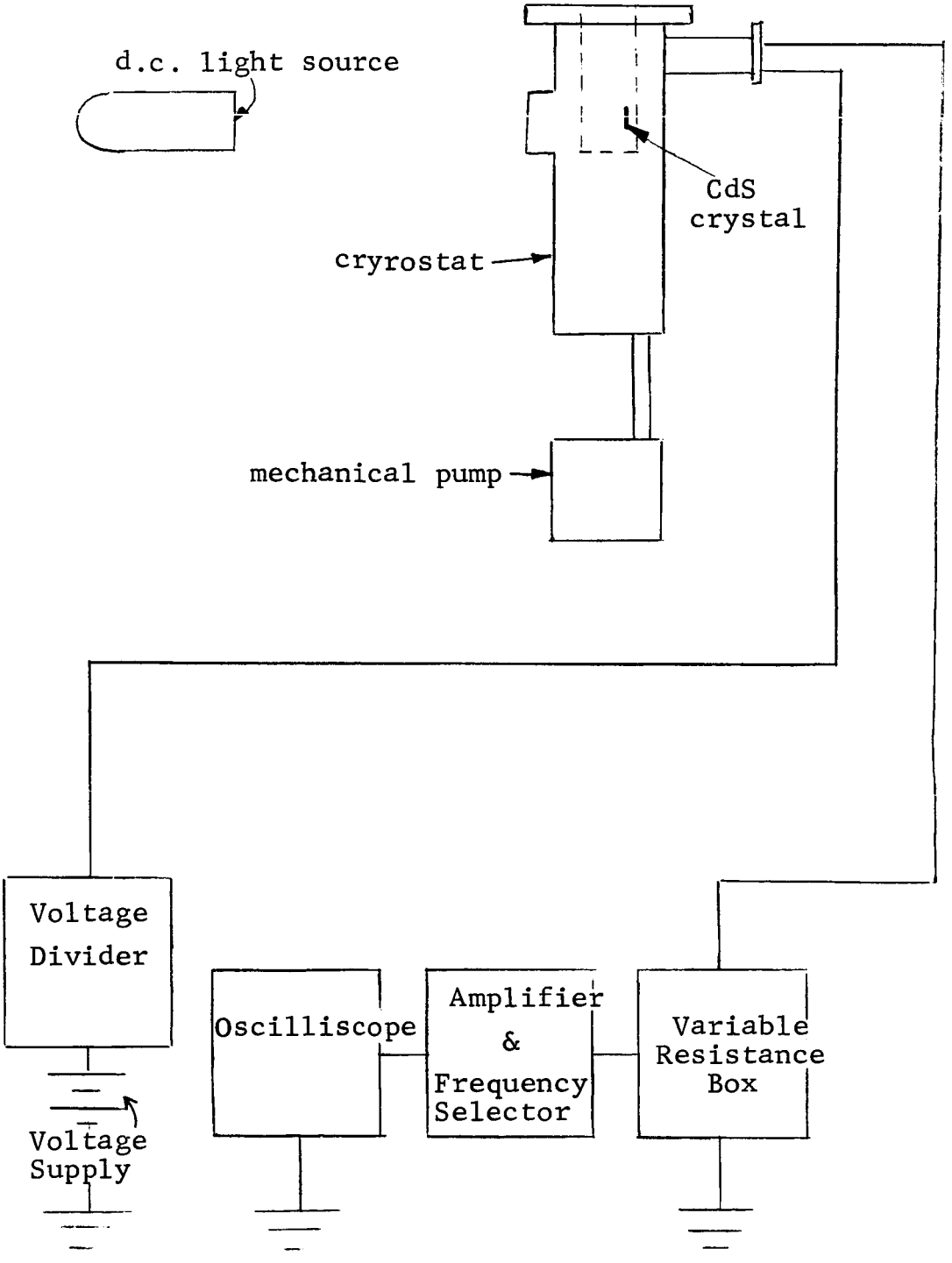

Figure (12). Schematic of apparatus used to measure contact noise.

V. EXPERIMENTAL RESULTS

A. Single layer electrodes. Several crystals were electroded using just a single metal. Generally, the findings substantiated previous data using this approach. In all cases an attempt was made to make the contacts opaque to light in order to avoid photoeffects due to photoemission of electrons from the metal into the CdS bulk.[19] All irradiation was done with green light.

1. Gold. The three samples with gold as the electrodes all exhibited non-ohmic characteristics at low voltages and current saturation at high voltages indicating blocking contacts. Figure (13) shows the I-V curve for a single layer gold electrode evaporated in an oxygen ambient. In this crystal with no applied voltage there was a very marked photo current-or photovoltage.[d] At zero applied voltage and a light intensity of $.1I_o$, a current was registered on the micro-micro ammeter. When the light was turned off the current went to zero. Then if the light was turned on at light intensity $.001I_o$, the photo-

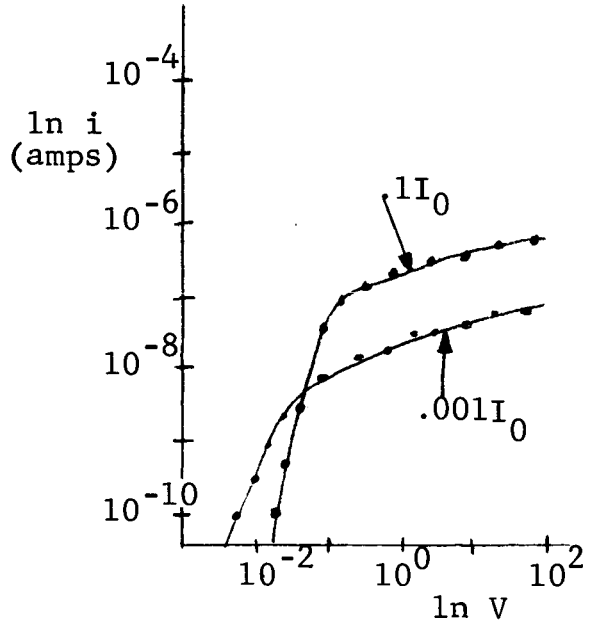

Figure (13). I-V curve for gold electrodes.

[d] The observance of a photovoltage would occur if the leads to the external circuit were infinite; if the leads (of the two electrodes) were shorted, a photo current would be read.

current returned but its magnitude was not as great as for the case of $.1I_o$ light intensity. When low voltages (less than 10mv) were applied to the crystal at a given light intensity, the current would decrease or increase depending on the polarity of the applied voltage. In the case of decreasing current with increasing low applied voltages, the current would pass through "zero current" and then start increasing in the opposite direction with further applied voltage. See Figure (13).

Figure (14) shows the I-V curve for one of the two crystals with gold electrodes evaporated in nitrogen ambient. In this case the I-V curves showed a definite saturation region followed by a greater than linear increase of current as a function voltage. Subsequent heat treatment at 100°C and 200°C resulted in little, if any, change in the I-V curves. This would seem to indicate that there was no diffusion of the gold into the CdS. A spectral response (photocurrent versus wavelength of irradiating light) curve was run on this crystal and showed a marked peak at 517 mμ (bandgap) for applied voltages at the crystal

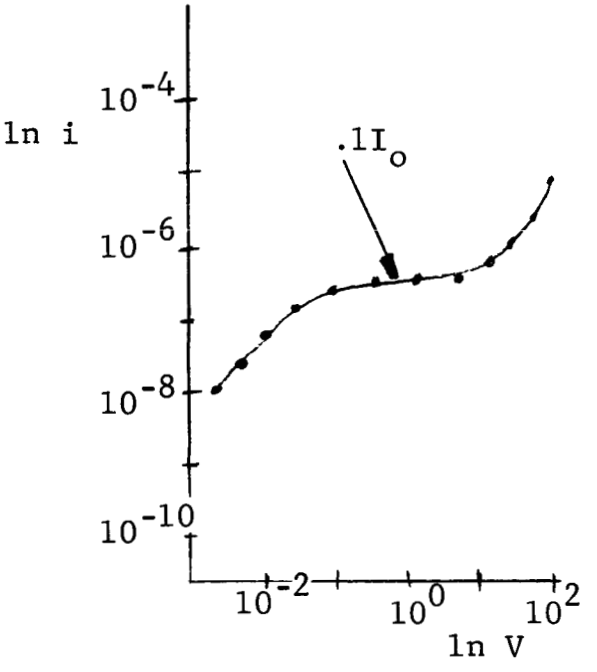

Figure (14). I-V curve for gold electrodes.

which were before and after the saturation region. The spectral response curve run at an applied voltage chosen in the saturation region showed little response at 517mμ.

2. Indium. Two crystals were electroded in a nitrogen ambient with indium as the contact. They both showed ohmic behavior in that the I-V curves were linear and the contact noise was fairly low. See Figure (15). Prior to heat treatment, rough photo-response measurements showed that for light intensity $.1I_o$ the current would, when the light was turned off, fall to .2 of its initial value in a time of 10 seconds. A heat treatment for 15 minutes with the crystal system at 100°C was done. Upon cooling slowly (about 4°C/min) the subsequent I-V curve for light intensity $.1I_o$ shifted up more than an order of magnitude and was still very linear. The response in 10 seconds from an initial light level of $.1I_o$ was to a value of much less than .1 of the initial current value. For an initial light level of $.001I_o$ the current fell to .2 its initial value in ten seconds after the light had been shut off. Also the I-V profile for $.001I_o$ light intensity after heat treatment

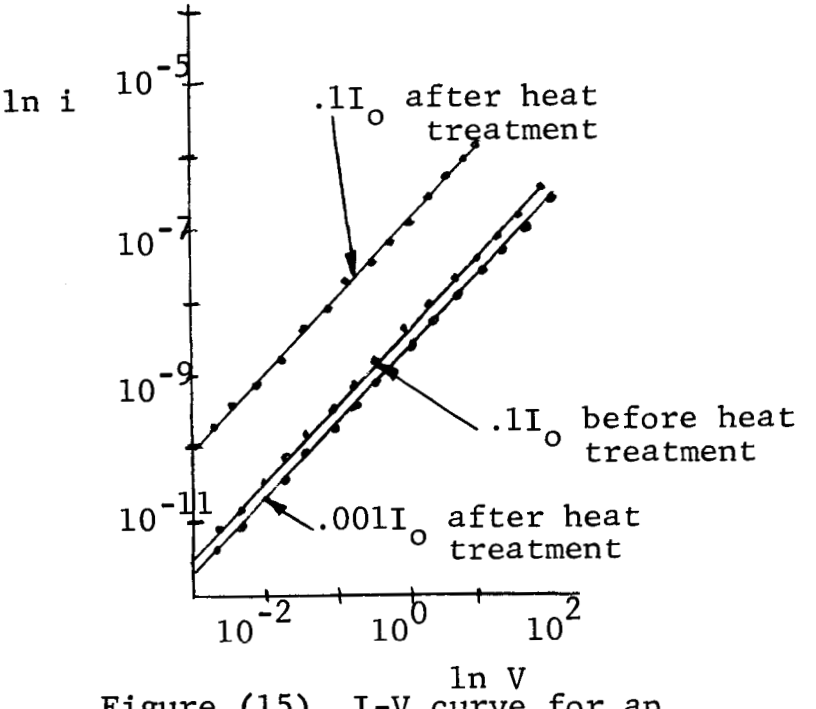

Figure (15). I-V curve for an indium electrode.

was approximately the same as the profile for the $.1I_o$ light intensity before heat treatment. This would indicate that there was possibly a diffusion of the indium into the CdS crystal, where acting as a donor,[13] it would raise the Fermi level and steady current at a given light level. This explanation of In acting as a donor and changing the Fermi level also would result in some kind of change in the response time as was observed.

3. Copper. A crystal with copper electrodes evaporated in nitrogen ambient was investigated and showed high contact noise and current saturation at high applied voltages. See Figure (16). This tendancy toward saturation occured at higher currents for higher light intensities. This phenomena was also observed by Ruppel[5].

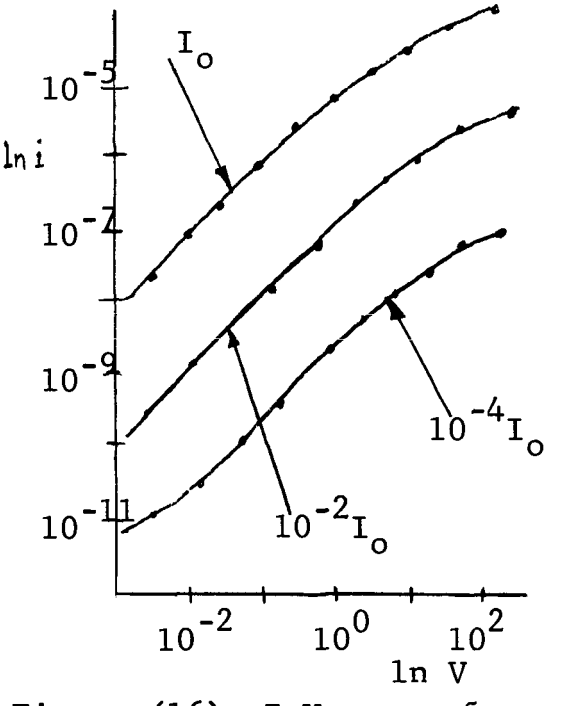

Figure (16). I-V curve for a copper electrode.

4. Aluminum. Five crystals were electroded in an air ambient with just a single deposition layer of aluminum as the contact. In two cases the electrical contacts were actually very good, showing no appreciable contact noise and excellent I-V characteristics. One crystal showed no current response as a function of voltage; it was also not photosensitive. Another non-ohmic behaving crystal shown in Figure (17) gave

an $I \propto V^n$ curve but did not have any photo-response at a light intensity of I_o until high applied voltages (average field at 10^2 volts/cm.).

On the other hand, two of the crystals using the aluminum electrodes showed, besides low contact noise levels, excellent I-V characteristics. See Figure (18). The crystals were extremely photosensitive, reacting to light levels as low as $10^{-7} I_o$ (an electron excitation rate of $\sim 10^9$ cm^{-3} sec^{-1}). Both crystals gave the space charge limited current effect (SCLCE) in that they would give a steep initial increase (greater than $I \propto V^2$) of current for an increase of voltage and then settle down to a steady state current value.[20] For light intensities from $10^{-7} I_o$ to $10^{-3} I_o$ the I-V profile was linear from

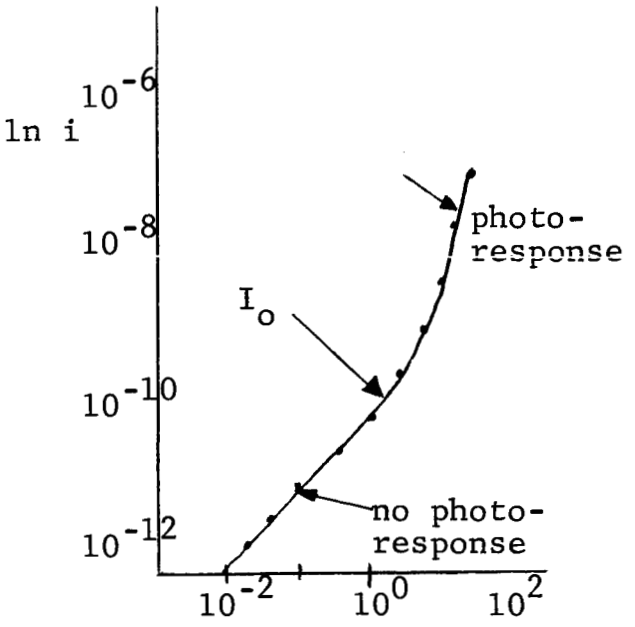

Figure (17). I-V curve for non-ohmic aluminum electrodes.

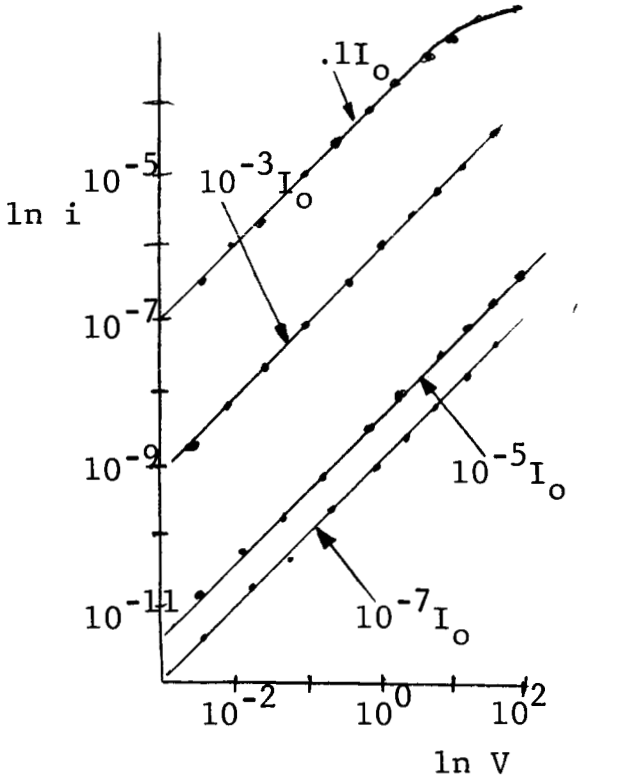

Figure (18). I-V curve for ohmic aluminum electrodes.

10mv to 400 volts. For a light level of $.1I_o$ the current began to saturate at about 10^{-3}amps at an applied voltage of 100 volts. This would indicate from j_o calculations using the diffusion theory a barrier height of .36ev.

5. Titanium.

Two crystals with titanium electrodes evaporated in nitrogen ambient gave fairly high contact noise, non-ohmic current behavior. As shown in Figure (19) the curve reached a saturation for light intensity I_o at about 10^{-4}amps/cm^2.

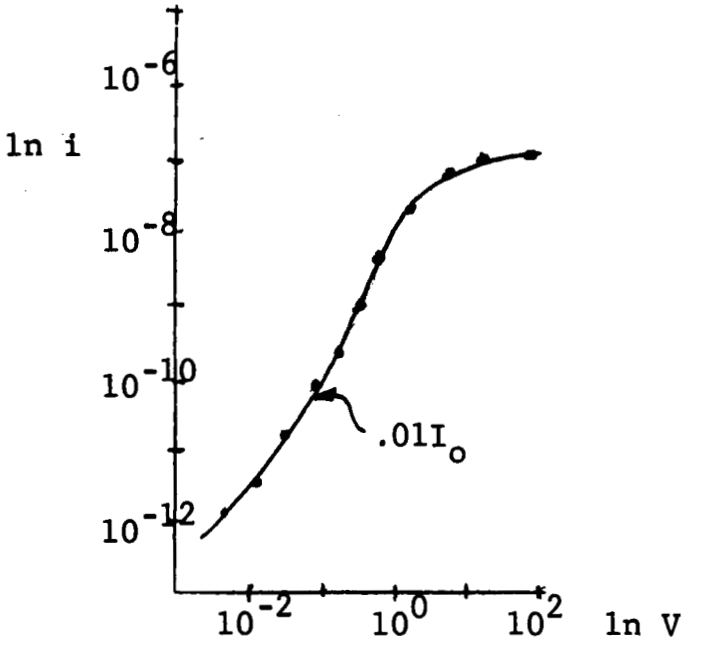

Figure (19). I-V curve for titanium electrodes.

B. Multi-layer electrodes. When multi-layer electrodes were evaporated, it was again attempted to make the contacts opaque to light in order to avoid photo-emission effects.

1. In-Au. Several crystals were electroded using indium as the active metal and gold as the covering metal. About 80% of these cases gave initially ohmic I-V curves with relatively low contact noise. Of those ohmic crystals that were heat treated, none appeared to remain stable (that is their I-V curves changed markedly, and in some cases contact noise increased.) For example, some crystals after heat treatment yielded a parallel shift in the I-V curve as shown in Figure (20). Other crystals yielded I-V curves after heat treatment which were generally lower than the preheated curves and which showed a definite saturation range. See Figure (21).

2. Au/Al. Several multi-layer electrodes were tried using gold as the preparative metal and Al as the active metal. The results were only fairly satisfactory. Three of the eight as shown in Figure (22) gave fairly low contact noise levels, and linear I-V profile. Two of the remaining five that were heat treated at $100^{o}C$ showed definite improvement from saturating I-V curves to fairly linear characteristics. See Figure (23). Further investigation into using these two metals turned out not to be beneficial. It was learned that between the simultaneous evaporation of gold and aluminum and the subsequent cooling of the metals on the CdS substrate, there was a phase transition.[21] This would create additional mechanical strain on the CdS crystals which would effect the crystal character in an undetermined fashion.

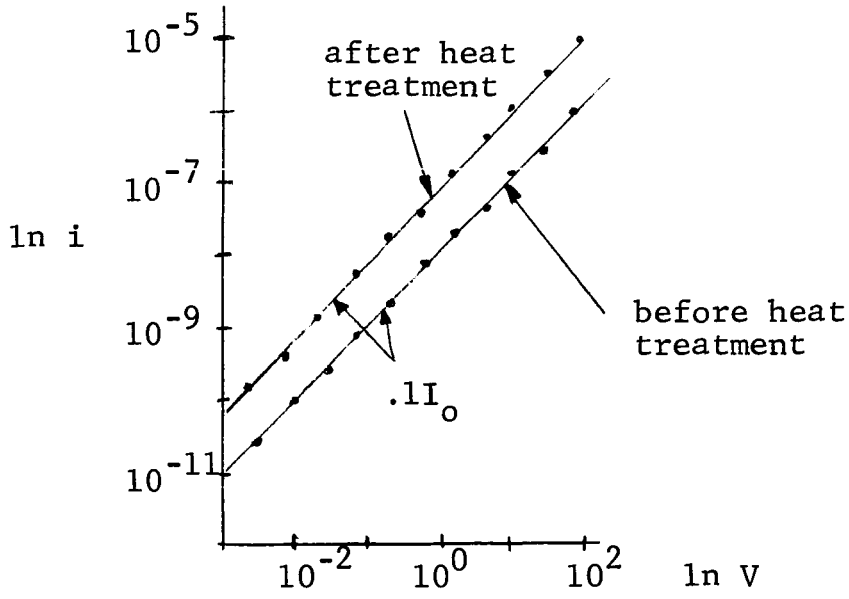

Figure (20). I-V curve for In-Au.

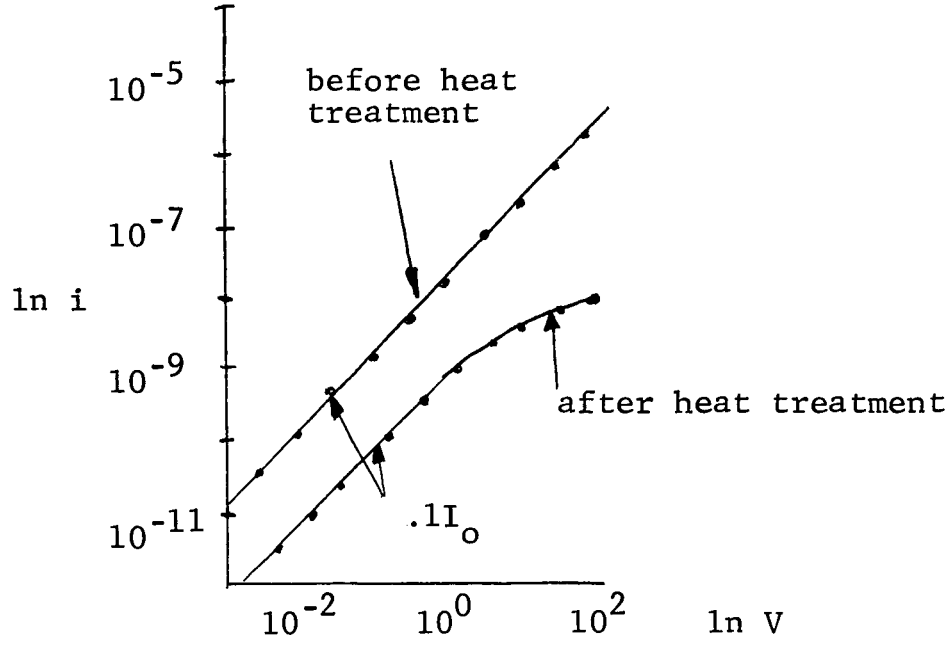

Figure (21). I-V curve for In-Au.

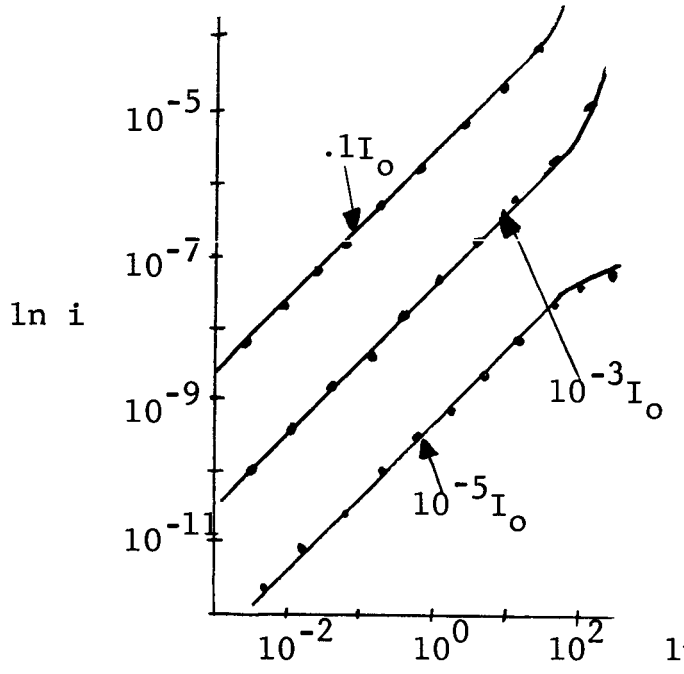

Figure (22). I-V curve for ohmic Au/Al electrodes.

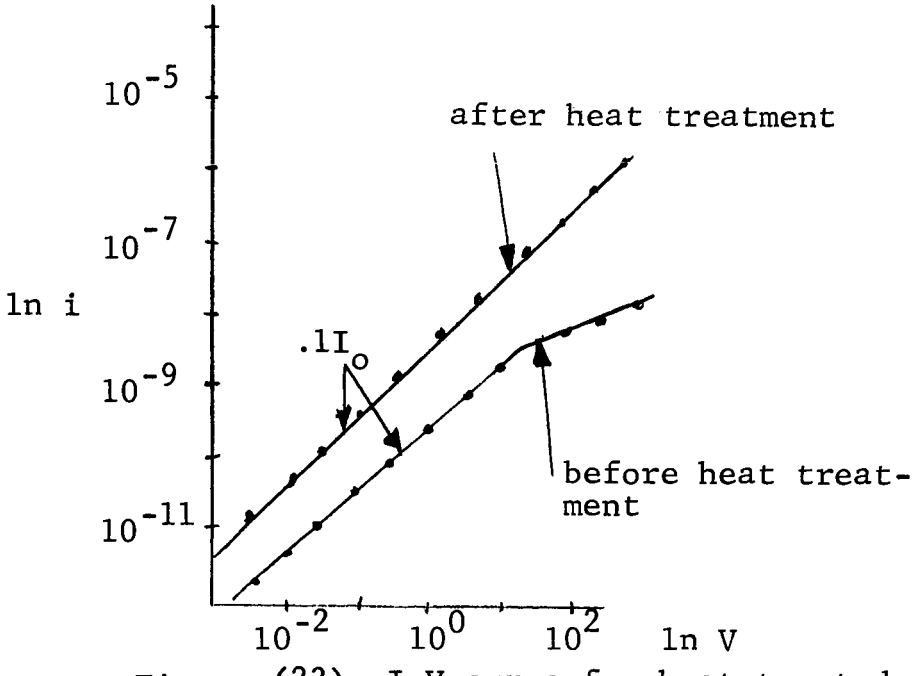

Figure (23). I-V curve for heat treated Au/Al electrode.

3. Ti/Al. The results using Ti and Al as the metals in the dual evaporation technique were the most satisfactory. All contacts using Al and titanium as the electrodes with Ar or N as the ambient turned out to behave ohmically. In about half the cases where Ar or N ambient gas was used in the evaporation procedure, heat treatment of the resulting electrodes-CdS crystal system was necessary. It was as a result of these crystals which needed heat treatment that the actual success of the dual evaporation procedure was indicated. In Figure (24) is shown I-V curves run on crystals having Ti-Al electrodes before heat treatment. Note that for two different light intensities the current shows a definite current saturation. Upon heat treat to 200°C and subsequent I-V measurements, the curve linearizes, and for the same light intensity shifts to higher current values-indicating a lower series bulk plus contact resistance. Also, after the crystal has been heat treated there is no saturation observed indicating a possible covering of the barrier height.

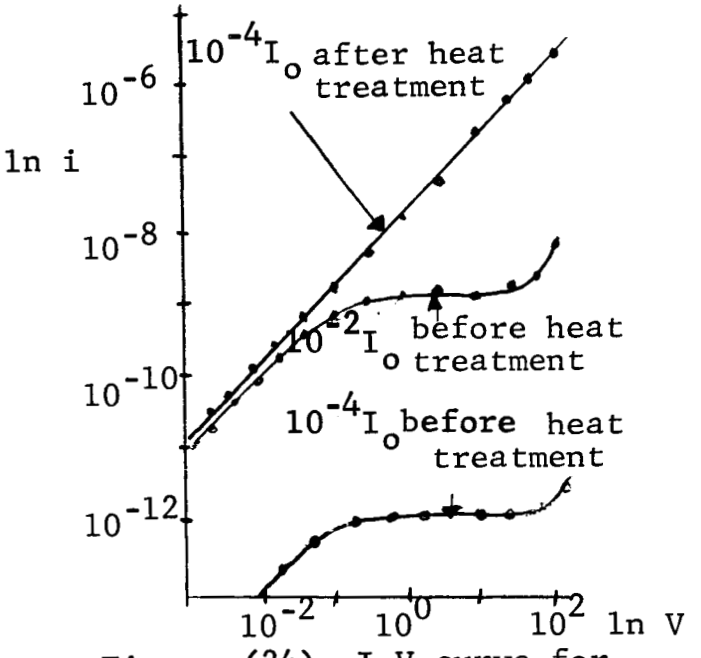

Figure (24). I-V curve for heat treated Ti/Al electrodes evaporated in nitrogen ambient.

In the cases when titanium and aluminum were evaporated as multi-layer electrodes in an oxygen ambient, the I-V curves were not ohmic. The I-V curves shown in

Figure (25) indicates the nonohmic behavior of the electrode before and after heat treatment. It should be noted that while there is a change in the curves as a result of heat treatment, the electrode still does not behave ohmically.

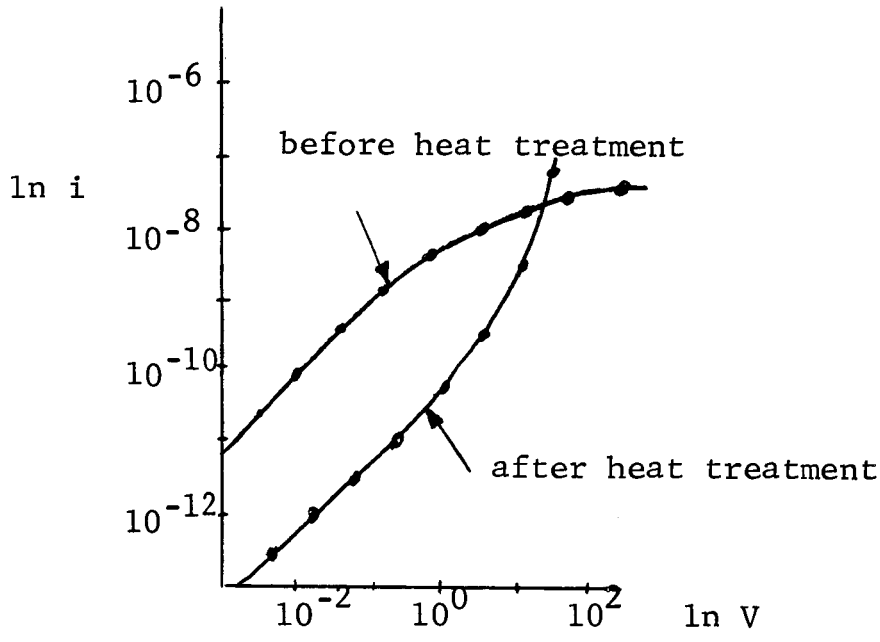

Figure (25). I-V curve for non-ohmic Ti/Al electrodes in oxygen ambient.

IV. DISCUSSION AND CONCLUSION

A. Discussion of Experimental Results. In analyzing the experimentally obtained I-V curves, use is made of the theoretical $\bar{I}$-$\bar{V}$ profiles developed in Chapter II. It is assumed that the field at the barrier is given by the linear approximation,

$$E_B = \frac{V_j}{w} \tag{31}$$

where: $V_j \equiv$ the voltage at the cathode junction
$w \equiv$ the effective barrier width (from consideration of Poisson equation). See equation (23).

The potential difference at the cathode is

$$V_j = \frac{\Phi_m - \Phi_s}{e} + V_{Aj} \tag{32}$$

where: $V_{Aj} \equiv$ that part of the applied voltage, V_A, which appears at the cathode junction.

Two supplementary conditions that can be applied are:

1) if $E_B > 10^6$ volts/cm. then barrier breakdown occurs.

2) if $w < 5 \times 10^{-6}$cm. then diode theory must be used.

When the breakdown voltage, V_{br}, is reached, then $E_B = 10^6$ volts/cm. (by assumption) and from equation (31)

$$E_B = 10^6 \text{ V/cm.} = \sqrt{10^{-7} N_d^*} \sqrt{V_j}. \tag{33}$$

If, for example, barrier breakdown occurs when the cathode is current saturated as shown in Figure (26) then $V_A = V_{Aj} = V_{Abr}$

and equation (32) becomes

$$V_j = \frac{\Phi_m - \Phi_s}{e} + V_{Abr} = V_{br} \qquad (34)$$

where: $V_{Abr} \equiv$ that applied voltage at which time barrier breakdown occurs.

Note that,

1) if $V_{Abr} < 100\text{mv}$ then $V_j \simeq \frac{\Phi_m - \Phi_s}{e}$

2) if $V_{Abr} > 10$ volts then $V_j = V_{Aj} = V_{br} = V_{Abr}$.

Thus equation (34) may be used in equation (33) to evaluate N_d^*. Using N_d^*, w can be calculated from equation (23). Then depending on whether w is greater than or less than 5×10^{-6} cm., the value of i_o in the I-V curve may be used in equation (3b) or (6b) to evaluate the barrier height, $\Phi_m - \chi$.

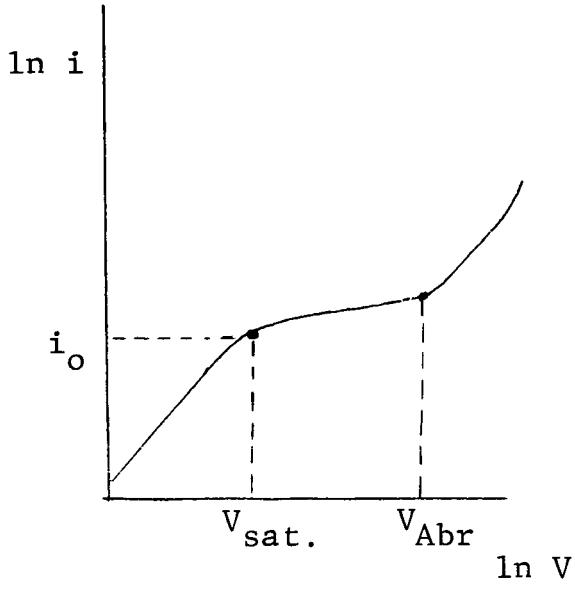

Figure (26). A theoretical I-V curve showing current saturation and barrier breakdown.

If on the other hand there is no V_{Abr} attained within the power dissipation limits of the crystal, it is still possible to get an indication of some of the junction quantities. First, if $V_{sat} > 100$ mv, then the I-V curve is bulk determined in the range of 1 mv. $< V_A \leq$ 100mv. Second, by using the largest value of V_A which neither exceeds the power dissipation limits of the crystal, nor causes a physical electrode

breakdown, values of what N_d^* must be less than can be obtained from

$$E_B < 10^6 \text{ V/cm} > \sqrt{10^{-7} N_d} \sqrt{V_j} \, . \qquad (35)$$

From this value of N_d^* it is possible to obtain values which w must be greater than.[e]

For example, consider the case of gold contacts which saturates at 5×10^{-5} amps/cm^2, have $V_{br} = 100$ volts, and V_{sat} occurs at 10^{-1} volts: from equation (33) one obtains,

$$10^6 = \sqrt{10^{-6} N_d^*}$$

$$\text{or } N_d^* = 10^{17} \text{cm}^{-3}$$

Then from equation (23) it follows

$$x_o = \sqrt{\frac{10^7}{N_d^*}} \quad \text{or} \quad x_o = 10^{-5} \text{cm}.$$

Thus since $x_o > 5 \times 10^{-6}$ cm, the diffusion theory is used to calculate $\Phi_m - \chi$ from $j_o = e\mu E_B N_c \exp(-(\Phi_m - \chi)/kT)$. This leads to

$$5 \times 10^{-5} = (10^{-19})(10^2)(10^6)(10^{19}) e^{-(\Phi_m - \chi)/kT}$$

and it turns out that: $\Phi_m - \chi = .747$ ev. which is in excellent agreement with other experimentally obtained values.[14, 15]

An additional analysis of an I-V curve for a crystal with gold electrodes was provided by consideration of the spectral response curve. The spectrals A) and D) as shown

---

[e] In evaluating w, it is the value w_T, the distance that an electron must go to get from the Fermi level of the metal into the conduction band of the semiconductor, that determines which theory - diode or diffusion-is to be used. The value of $x_T \sim \sqrt{2\varepsilon/eN_d^*}$.

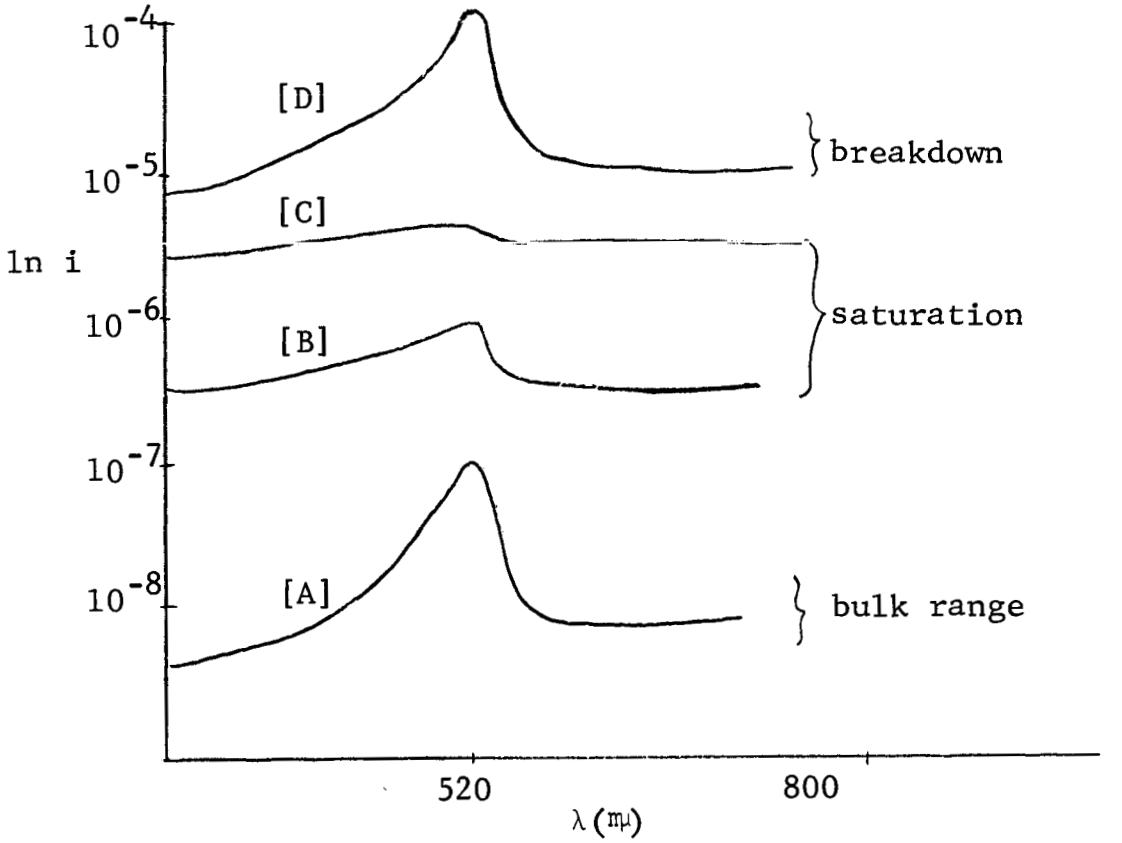

Figure (27). Spectral response curves such as a function of applied voltage.

in Figure (27), which were obtained for applied voltages occurring before and after the saturation region of the I-V curve, show a pronounced peak at 520 mμ. For the spectral curves B) and C) the voltages chosen were in the saturation region; note that the peak at 520 mμ is markedly reduced. This effect occurs since during the current saturation region, practically all the applied voltage exists at the junction, thus preventing a bulk response to the bandgap light.

The two different changes in the In-Au I-V curves after heat treatment may probably both be attributed to indium diffusion. In the cases which after heat treatment showed a parallel shift in the I-V curve, it is very probable that the active layer of indium was too thick (i.e. more than a monolayer) hence the heat treatment enhanced diffusion of

the excess indium into the bulk. In the other case after heat treatment the I-V curve shifted down and showed a definite saturation. It seems that initially the indium formed an ohmic contact to the CdS, however after heat treatment the indium at the CdS surface was replaced by gold which lead to a high resistance contact that saturated at high voltages.

The use of aluminum or titanium as evaporated electrodes proved generally unsuccessful; that is, none of the evaporated Ti electrodes showed ohmic behavior, and only two of the evaporated Al electrodes were ohmic. In one case in which an evaporated aluminum electrode turned out to be non-ohmic, there was no photo-response at low voltages from 1 mv to about 1 volt using light intensity, I_o. However, at higher applied voltages ($>$ 10 volts) there was a photo-response. This would seem to indicate that there was a high barrier layer at the surface which at low voltages dominated the circuit, but which at higher voltages "broke down" resulting in $I \propto V^n (n>1)$; now the bulk crystal dominated the circuit and a photoresponse was measurable.

The change in several of the Ti/Al I-V curves at a given light intensity from low current values and saturation before heat treatment to higher current values and no saturation after heat treatment, leads to two possible explanations. First, since aluminum acts as a donor in CdS, diffusion of aluminum into the crystal would reduce the contact resistance and cause an effective barrier lowering. A second possibility is that the heat treatment causes the aluminum to make a relatively intimate contact with the CdS, thus creating a low resistant contact.

One interesting phenomenon observed was the variation of crystal response time as a function of voltage. Measurements on several crystals having non-ohmic currents showed

that an increase in voltage led to a decrease in response time, τ_r. In contrast crystals with linear I-V curve yielded constant, response times as a function of voltage.

Since this phenomenon was observed only on crystals which exhibited I-V profiles where $I \propto V^n$ (with $n \leq 1$), it is possible to explain this effect by considering an injected charge at the cathode. Thus by using an expression for response time given by[22]

$$\tau_r = \frac{N_t}{a} \tag{36}$$

where: $N_t \equiv$ number of traps/cm^3 existing within a kT energy of the quasi Fermi level, E_{fn}.

$a \equiv$ excitation rate of electrons,

it is seen that if some of the injected charge becomes trapped changing the quasi-Fermi level, then

$$\tau_{r1} = \frac{N_{t1}}{a}$$

$$\tau_{r2} = \frac{N_{t2}}{a} \tag{37}$$

where: $N_{t1} \equiv$ density of traps existing within a kT energy of the quasi Fermi level, E_{fn1}

$N_{t2} \equiv$ density of traps existing within a kT energy of the quasi-Fermi level, E_{fn2}.

If $N_{t2} > N_{t1}$, it would follow that $\tau_{r2} > \tau_{r1}$. Thus a change in the quasi-Fermi level due to the trapped injected charge would give rise to a voltage dependent response.[f]

---

[f] The meaning of equation (36) is as follows: if the quasi-Fermi level lies at a level of density N_t, then when the light excitation is turned, the photocurrent will fall to 1/e of its initial in the time τ_r.

The effect of flushing the vacuum system prior to evaporation was quite marked. Flushing with nitrogen and argon enhanced the sucess of the multi-layer technique relative to those times when air or oxygen were used. The exact mechanism by which the oxygen effect is reduced as a consequence of the nitrogen or argon flushing is not completely understood. If the gas used for flushing merely replaced the "air" present in the system, it would be expected that, due to pumping rates, the effects of changing the ambient would disappear within minutes; the vacuum being determined by the outgassing of virtual leaks. The fact that there is a definite influence seems to indicate some exchange taking place at the last few adsorbed layers on the walls of the vacuum system and on the surface of the CdS crystal (e.g. nitrogen for oxygen).

B. General Comments. In interpreting the results there was a certain amount of difficulty encountered because of the electrode configuration. Figure (28) shows schematically the field and equipotential lines of such an electrode

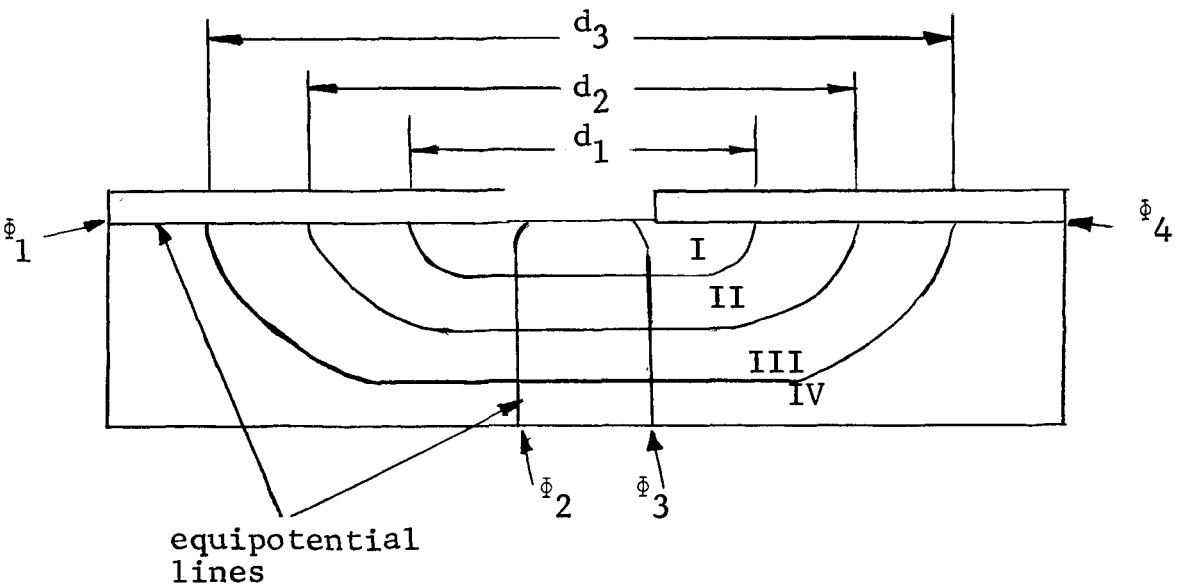

Figure (28). Schematic of field and equipotential curves for the electrode configuration used in the experiments.

configuration. As a result of potential considerations the current density will be lower in region IV than region I, thus making it difficult to identify and interpret any space charge limited currents (i.e. V^2/d^3) that might exist. Since the voltage, $d\Phi = \Phi_1 - \Phi_4$, does not depend on the region being considered, each region has a different d associated with it such that

$$i_1 = \frac{V^2}{d_1^3} > i_2 = \frac{V^2}{d_4^2} \quad . \tag{38}$$

Thus, if it assumed that the current is carried through the bulk and not on the surface, any current reading may be a combination of space charge limited currents and ohmic currents.

Also, due to the electrode configuration it is difficult to precisely determine current saturation since current requirements for the various regions are different; thus one region of the electrode would tend to saturate before another.

A discussion of electrical resistance in the contact region is difficult as was demonstrated by Sal'kov and Sheinkman.[23] They showed by using photosensitivity measurements that an increase in photosensitivity in the regions adjacent to the electrodes was due to severe inhomogeneity of the actual contact of the metal to the CdS. For their case then, the effective cross sectional area of the semiconductor at the contacts was less than the cross sectional area in the midportion. In the electrode configuration shown in Figure (28) this effect would make the electrode "area" approximately equal in magnitude to the cross sectional area of the bulk crystal.

The question also arises as to the effect at the junction after barrier breakdown has occurred. It is hard to conceive that a field breakdown effect would be reversible,

yet after an initial the I-V curve is run, all ensuing curves are generally reproducible - even the $I \propto V^n$ range that occurs after the saturation. It seems likely, therefore, that any physical change in the junction would have to be for a very small area of the electrode such that the actual resistance of the affected region would be large. This type of localized region effect could occur at a section of the metal-semiconductor interface which had a higher resistivity. After breaking down, the localized region would have a high conductivity, permitting the additional electron flow from metal into the semiconductor. How this localized region breakdown effect would allow reproducible I-V curves (i.e. still overall blocking contact behavior at low voltages) is still an open question.

It is recommended that in the future the CdS substrate be heat treated in vacuo before depositing the multi-layer electrodes. As Böer and Lubitz have discussed in their paper, this procedure serves to enhance favorable conditions for creating ohmic contacts.[g]

Generally, the multilayer technique suggested by Böer is successful in creating heat resisting, ohmic behaving contacts to CdS single crystals. In the experiments performed

---

[g] As it turns out, heating the CdS substrate not only rids the surface of contaminants (oxygen, etc.) but also influences the ensuing metal layer deposit. Studies have shown that condensing atoms (of the metal) tend to take on the structure type of the substrate, forming amorphous layers on amorphous substrates and single crystal layers on single crystal substrates. This behavior is temperature dependent in such a way that at room temperatures the films are amorphous and at higher temperatures the films tend toward being monocrystalline.[17] Thus, since the emission energy is less for the amorphous crystal than for the single crystal, it would be desirable to cool the CdS substrate before depositing the electrode layers.

the greatest success was attained using Diemer's suggestion of titanium with aluminum; the key being to deposit only enough titanium (< 15 Å) such that its presence does not dominate the junction characteristics.

REFERENCES

1. Spenke, E. Electronic Semiconductors. McGraw Hill Book Company, Inc. New York. 1958. p. 81.
2. Mott, N. F. and Gurney, R. W. Electronic Processes in Ionic Crystals. The Clarendon Press. Oxford. 1940. p. 172.
3. Rose, A. Physical Review. 97. 1538 (1955).
4. Lampert, M. A. Physical Review. 103, 1648 (1956).
5. Ruppel, W. J. Phys. Chem. Solids. 22, 199 (1961).
6. Butler, W. and Muscheid, W. Ann. Phys. 14, 215 (1954), 15, 82 (1954).
7. Fassbender, J. Z. Phys. 145, 310 (1953).
8. Smith, R. W. Physical Review. 97, 1525 (1955).
9. Smith, R. W. R.C.A. Review. 12, 350 (1951).
10. Walker, W. and Lambert, E. I. Journal of Appl. Phys. 28, 635 (1957).
11. Sihvonen, I. T. and Boyd, D. R. Journal of Appl. Phys. 29, 1143 (1958).
12. Böer, K. W. and Lubitz, K. Zeit. Fur. Natur. 17a, 397 (1962).
13. Diemer, G. Philips Res. Rep. 10, 194 (1955).
14. Spitzer, W. G. and Mead C. A. Journal of Appl. Phys. 34, 3061 (1963).
15. Goodman, A. M. Journal of Appl. Phys. 35, 573 (1964).
16. Böer, K. W. personal communication.
17. Heavens, O. Optical Properties of Thin Solid Films. Butterworths Scientific Publ. London. 1955. p. 8.
18. Mac Farlane, G. G. Proc. Phys. Society of London. 59, 366 (1947).
19. Williams, R. and Bube, R. H. Journal of Appl. Phys. 31, 968 (1960).
20. Smith, R. W. and Ruse, A. Physical Review. 97, 1531 (1955).
21. Hansen, M. Constitution of Binary Alloys. McGraw Hill Book Co., Inc. New York. (1958). p. 68.

22. Rose, A. Concepts in Photoconductivity and Allied Problems. John Wiley & Sons, Inc. New York. 1963. p. 20.

23. Sal'kov, E. A. and Sheinkman, M. Soviet Physics-Solid State. 5, 172 (1963).